Synthesis and Characterization of Cu and Se Doped TiO_2 Photocatalysts and their Applications Against Glyphosate and Methyl Orange

A thesis submitted to the Department of Chemistry, School of Natural Sciences NUST, Islamabad, in partial fulfillment of the requirements for the degree of

Masters of Science (MS)

in

Chemistry

Submitted by: Zaib-un-Nisa

Reg No. NUST-201463666MSNS78214F

Supervisor: Dr. Habib Nasir

School of Natural Sciences (SNS)

National University of Sciences and Technology (NUST)

H-12 Campus Islamabad

2017

FORM TH-4

National University of Sciences & Technology

MS THESIS WORK

We hereby recommend that the dissertation prepared under our supervision by: ZAIB UN NISA, Regn No. NUST201463666MSNS78214F Titled: Synthesis and Characterization of Cu and Se Doped TiO2 photocatalysts and their Applications Against Glyphosate and Methyl Orange be accepted in partial fulfillment of the requirements for the award of **MS** degree.

Examination Committee Members

1. Name: DR. M. FAHAD EHSAN Signature: _____

2. Name: DR. MUHAMMAD ARFAN Signature: _____

3. Name: _____ Signature: _____

External Examiner: DR. TARIQ MAHMOOD Signature: _____

Supervisor's Name: PROF. HABIB NASIR Signature: _____

_____ Head of Department

18-10-17 Date

COUNTERSINGED

Date: 18/10/17

Dean/Principal

THESIS ACCEPTANCE CERTIFICATE

Certified that final copy of MS thesis written by **Ms. Zaib un Nisa**, (Registration No. **NUST201463666MSNS78214F**), of **School of Natural Sciences** has been vetted by undersigned, found complete in all respects as per NUST statutes/regulations, is free of plagiarism, errors, and mistakes and is accepted as partial fulfillment for award of MS/M.Phil degree. It is further certified that necessary amendments as pointed out by GEC members and external examiner of the scholar have also been incorporated in the said thesis.

Signature: _____

Name of Supervisor: Prof. Habib Nasir

Date: 18-10-17

Signature (HoD): _____

Date: 18-10-17

Signature (Dean/Principal): _____

Date: 18/10/17

Dedication

Dedicated to my beloved parents

Acknowledgements

All praise goes for **Allah Almighty** who gave me such abilities to think and work logically and gave me determination, resoultness and perseverance to accomplish this research project.

My gratitude extends to my sincere and helping supervisor **Dr. Habib Nasir** who gave me every possible opportunity and spent precious hours in pursuit to accomplish the project. He has been the source of inspiration and his support is an encouragement for me. Special thanks to my guidance and evaluation committee members **Dr. Muhammad Fahad Ehsan** and **Dr. M. Arfan** for their valuable guidance, suggestions and encouragement. I would also like to thank my mentor **Dr. Umair Manzoor**, HoD Materials Enginnering, SCME, NUST. I cannot overstate the importance of his contribution in my project work.

I pay respect and sweet sensation of love to my family especially my parents for being so supportive and understanding it would not have been possible to complete this project without their enormous support.

I would also like to thank my colleagues and friends **Tehreema Nawaz**, **Saba Bashir** and **Sumia Gul** for being there whenever I needed them. I always cherish happy moments spent with them.

Special thanks go to SCME, NUST, USPCAS-E, NUST and AIOU Islamabad for giving me opportunity to analyze all samples through various techniques, without their coorporation this project wouldn't have been completed**.**

Zaib-un-Nisa

Abstract

Advanced oxidation process in which TiO_2-Catalyzed UV Oxidation reactions has emerged as promising wastewater treatment technique. TiO_2 is most efficient photocatalyst because of its low dielectric properties, inert and chemically stable nature. In this thesis TiO_2 in pure anatase phase was synthesized by using sol-gel method which is highly efficient and used to obtain purity of samples. After that to reduce band gap of TiO_2 nanoparticles they were doped with Cu and Se ions in different ratios i.e. 1%, 3%, 5%, 7%, and 10 wt%. Precursors used for synthesis were TTIP, $CuSO_4.5H_2O$ for Cu doping and SeO_2 for Se doping. The nanocatalysts were characterized by XRD to find purity and phase, SEM for morphological analysis, BET to check surface area and pore size and EDS to determine the elemental composition. The Tauc plots were determined by taking absorbance from UV-Vis spectroscopy. Tauc plots of doped catalysts were significantly lesser than pure TiO_2 which was due to introduction of impurity energy levels in TiO_2 lattice. The degradation studies were carried out in presence of visible light using LEDs. Degradation studies of methyl orange and glyphosate were carried out using both the Cu doped TiO_2 and Se doped TiO_2. XRD spectra showed that crystallite size was decreased gradually from 21 nm to 11 nm as dopant level was increased and particle size was also reduced from 61 nm to 36 nm by adding different amounts of dopant. Efficiency of all the doped nanocatalysts were measured by taking absorbance after regular intervals of 3, 6, 9, 12 and 15 hours. And it was observed that doped samples of both Cu and Se series were showing better photocatalytic activity as compared to TiO_2 NPs. And comparing all the doped samples, nanocatalysts with dopant concentration of Cu-7% and Se-7% were the best among all the other catalysts. Between the Cu-7% and Se-7% catalysts, Cu-7% was better than Se-7%. Reusaability of Cu-7% doped nanocatalysts was also studied and it was observed that these catalysts can be reused for atleast 3 times with more than 75% activities.

List of Abbrevations

BET	Brunauer-Emmett-Teller
EDX	Energy Dispersive X-Ray Spectroscopy
eV	Electron volt
g	Gram
GLY	Glyphosate
Hrs	Hours
mg	Milligram
Mins	Minutes
MO	Methyl orange
Nps	Nanoparticles
SEM	Scanning Electron Microscopy
TiO_2	Titanium dioxide
UV-Vis	Ultra Violet-Visible Spectroscopy
VB	Valence band
XRD	X-Ray Diffraction

Table of Contents

List of Figures

List of Tables

List of Schemes

Chapter 1: Introduction

Our environment is continually evolving but as environment is changing so does the problems related to it. With uncertain weather patterns, influx in natural disasters and much more it is very important to be aware of all these problems and their consequences. Pollution is one of the major problems our Earth is facing now a days.

1.1. Pollution

1.1.1. Environmental pollution

Pollution is defined as the presence of the substance or its introduction into the environment causing poisonous or harmful effects.

Air, water and soil are polluted by chemical compounds and their bi-products. Agricultural and industrial wastes pollute the water that is harmful for human, plants and animals. Different human activities like deforestation, mining, littering and construction deteriorate the earth's surface causing land pollution. Hazardous smoke from industries, traffic, burning of fossil fuels and tanneries directly pollutes the air.

When we talk about environmental pollution we are basically talking about the three main environmental components namely water, soil and air. They may cause short term (acute) or long term (chronic) harm to the ecosystem. Environmental pollution may be anything which affects the hydrosphere, the lithosphere and atmosphere – or water, soil and air. Pollutants may be chemical in nature and their results could also be harmful physical phenomena i.e. greenhouse gases leading to global warming [1].

In Pakistan the pollution problems have been rising since it got its independence. Of the Pakistani cities Karachi, Peshawar and Rawalpindi are among the 20 most polluted cities in the world. As per the most recent statistics from the world health organization (WHO) compiled from more than 1600 cities for the year 2008-2013. So it's very important to understand reason of pollution and to develop methods to reduce it [2].

1.2 Types of pollution

Mainly there are five types of pollution:

1. Soil pollution
2. Water pollution
3. Air pollution
4. Noise pollution
5. Light pollution

1.3 Soil pollution

Soil pollution is the degradation of soil because of human or natural activities. Soil has direct contact with life on earth so its contamination also risks health. Various chemicals like polynuclear aromatic hydrocarbons, lead, heavy metals, organic solvents, pesticides and dyes are main causes of human main soil pollution. These chemicals are most common cause of pollution because they are very persistent and generally accumulate in the subsoil layer [3].

1.4 Water pollution

Water pollution occurs when pollutants directly and indirectly ejected into water bodies like rivers, lakes, oceans and ground water [4]. In Pakistan over 16 million people don't have access to clean drinking water. 250,000 children die every year of water borne diseases. Recent studies show that agricultural lands have very large amount of phosphorous (P) and nitrogen (N) transported through streams and river pathways [5]. Pakistan stands at 80 among 122 nations in world drinking water problems ranking [6].

1.5 Sources of water pollution

Sources of water pollution can be of two main types. Point sources which comes from single and identifiable source like domestic sewage, industrial effluents and mining etc. Other one is non-point source or sometimes referred as diffuse pollution in which we cannot define single source e.g. agricultural land in which pesticides, fertilizers, animal manure and soil washed into streams due to rainfall all are non-point sources [7]. Sources of water pollution can be in form of physical or chemical pollutants like change in temperature, large objects that are visual, dyes that change colour of water or pesticides that are colourless but cause hazardous effects on human and aquatic life. Studies have shown that in USA the amount of

Fertilizers using nitrogen and phosphorous in their contents are increased 20-fold from 1945-1993 [8] and nitrogen is main source of pollution. In asia major source of water pollution are organic matter, heavy metals, deforestation, eutrophication and pathogens [9].

1.6 Ways to remove water pollution

Due to excessive use of pesticides and their ability to remain in environment for longer periods of time they cause harmful effects on human health and environment. The notion of "less is good, more is even better" causing farmers to use pesticides above their normal prescribed doses. So this consistent and excessive use causes serious health problems. It is highly required to develop an efficient and economical way to remove organic pollutants and pesticides from waste water [10].

To treat waste water physical, chemical and biological treatment methods are used earlier.

1.7 Biological treatment method

Biological treatment methods rely on microorganisms such as bacteria, earthworms, nematodes and other microorganisms to degrade the pesticides and other organic pollutants into less harmful substances. In this method organic wastes can be treated in two ways using aerobic and anaerobic microorganisms [11].

1.8 Anaerobic treatment method

Anaerobic treatment includes use of bacteria in oxygen free environment which cause deterioration of organic material. Best example of anaerobic treatment is anaerobic digestion. Other methods are lagoons and septic tanks.

1.9 Aerobic treatment method

It includes degradation of organic material in presence of oxygen by microorganism to convert organic pollutants into carbon dioxide, water and biomass. Important aerobic treatments are aerobic digestion and activated sludge. Aeration system is very important during aerobic treatment to maximize oxygen supply and to minimize odors coming from waste water. Advantage of aerobic treatment method is that during degradation of organic material biogas is produced which can be used as fuel [12].

Following four main aerobic biological technologies are commonly used now-a-days

1. Conventional activated sludge process (ASP) system
2. Cyclic activated sludge system (CASS)
3. Integrated fixed film activated sludge (IFAS) system
4. Membrane bioreactor (MBR)

Disadvantage of biological treatment method is that as these pollutants are harmful and less biodegradable so they may kill or decrease the efficiency of microorganisms. During aerobic treatment large amount of sludge or waste is produced which is another problem while anaerobic treatment is not that efficient to use against pollution [13].

1.10 Physical treatment method

1.11 Sand filtration

Many layers of sand having different size are used as filter.Waste water flow through these layers separating the solid particles.

1.12 Screens

Screens like burlap cloth or wire are flexible or rigid screens to separate solid particles.Other than these two basic filtration techniques these are of many types

1. Microfiltration: Use to filter particles in size range of 0.1-1.5 μm.
2. Ultrafiltration: filter the particles in size range of 0.005-0.1 μm.
3. Nano-filtration: filter the particles in size range of 0.0001-0.00 μm.
4. Reverse osmosis: remove particles in size range of upto 0.001 μm [14].

1.13 Chemical methods

Chemical methods include following main treatment methods:

1.14 Clarification

This method is effective in removing large particles but small size particles remain unseparated. So after clarification other treatment methods are needed to clean water completely.

1.15 Deionization and softening

Polluted water also known as hard water contain calcium and magnesium ions. So water softener are used which cause ion exchange by removing these ions producing deionized water.

1.16 Chlorine disinfection

To kill microorganisms like bacteria and pathogens chlorine disinfectants are commonly used. But these disinfectants cannot degrade the organic pollutants. Best and most effective way to remove the organic pollutants is by degrading them is using oxidation-reduction reactions. A method “Advanced oxidation process” was developed that form highly reactive species which further degrade the pollutants [15].

1.17 Advanced oxidation process

Advanced oxidation process is set of chemical oxidation reactions involving $OH^{\bullet}$ radicals for successful degradation of carcinogenic, harmful and bio-resistant chemicals. They degrade without creating secondary pollution. The $OH^{\bullet}$ radicals have highest oxidation potential after fluorine and have a rate constant of 10^6-10^9 $mol^{-1}L^{-1}s$. It means they attack all organic compounds very fast. $OH^{\bullet}$ radicals are also suitable for AOP’s because of its high versatility, can be produced by many possible ways like reaction with H_2O_2, using UV or just vis irradiations, by using H_2O/O_3/UV or O_3/UV and have highest thermodynamic oxidation potential having first order kinetics. Oxidation potential of $OH^{\bullet}$ radical is 2.80 so they have potential to oxidize almost every organic molecule converting them into less harmful inorganic ions and CO_2 [16].

1.2 Nanocatalysts

Nano catalysts are actually catalysts having nanoparticle size ranging from 1-100 nm. Nano catalysts are preferred because of their 100% selectivity, very high activity, long lifetime, low energy requirement and their reusability. Nano catalysts can be heterogeneous, homogenous and enzymatic in nature. Heterogeneous catalysts include nanoparticles of semiconductors, metals, oxides and some other compounds. Heterogeneous catalysts are solid and dispersed in matrix often forming suspension so they can be easily filtered after use and friendly as well. While on the other hand homogenous catalyst are used in a medium as

reactants. They have advantage of high selectivity but they cannot be recovered and poses major threat to the efficiency of process [17]. They can be destroyed by incineration but that adds some extra steps to the overall process.

1.2.1 TiO_2 Semiconductor

There are different materials with semiconducting properties like SnO_2, GaAsP, GaP, ZnO, CdS, WO_3, CdSe, GaAs, SiC, and TiO_2. For better photo catalytic activity the band gap of semi-conductor should lie in the range of reduction potential. TiO_2 has band gap of 3.20 eV and lies exactly in the range of reduction potential so it can be used in photocatalysis [18]. TiO_2 is used because of its large scale properties as they are very stable, chemically inert, UV active, non-toxic, high reduction potential of 2.4538, inexpensive, has dielectric properties and strong adsorption capacity. Moreover its surface acts as both Lewis acid and base making it an efficient material to degrade [19]. Mechanism of photo degradation works in a way that in the presence of UV-light TiO_2 surface produces holes and electrons. Holes take part in oxidation reaction at top energy level of band gap and convert toxic substances into CO_2 while energy level at bottom of conduction band take part in reduction reactions with the help of electrons [20]. Some important chemical and physical properties of TiO_2 are as shown in **table 1.1.**

TiO_2 has vast applications like solar cells, anti-fogging mirrors, sun screen creams, skin protecting cream, anti-bacterial material, sewage treatment, photo catalyst, cleaning ceramics, food packing material, paper making industry, coating, printing ink and staining pottery.

TiO_2 has three forms anatase, rutile and brookite as shown in **fig 1.1.**

Anatase: Anatase is best suited for photocatalytic activity because of low dielectric constant, high electron mobility and lower density. Anatase has Fermi level a bit higher that's why it has ability of high hydroxylation and less ability to absorb oxygen. It has band gap of 3.2 eV, tetragonal structure and more stable than rutile at 0K.

Rutile: Rutile has band gap of 3.02 eV and tetragonal in structure. Rutile is more stable than anatase and brookite if particle size is more than 14 nm. As a photo catalyst rutile doesn't show appreciable activity but they can be used in sunscreens, paints and dyes.

Table 1.1. Characteristics of TiO_2 [21].

Symbol	**TiO_2**
IUPAC names	Titanium dioxide, Titanium (IV) oxide
CAS no	13463-67-7
Elements present	Titanium, Oxygen
Electronic configuration	Titanium [Ar] $3d^2$ $4s^2$ Oxygen [He] $2s^2$ $2p^4$
Density	4.23 g/cm^3
Molar mass	79.9378 g/mol
Odour	Odourless
Appearance	White solid
Solubility in water	Insoluble
Band gap	3.05 eV
Refractive index	2.488
Magnetic susceptibility	+5.9 x10^{-6} cm^3/mol
Melting point	1843 ^oC
Boiling point	2972 ^oC

Brookite: It has band gap of 2.96 eV and orthorhombic crystal structure. It has large cell volume and more complicated as compared to rutile and anatase. Its efficiency is not good as a photocatalyst [22].

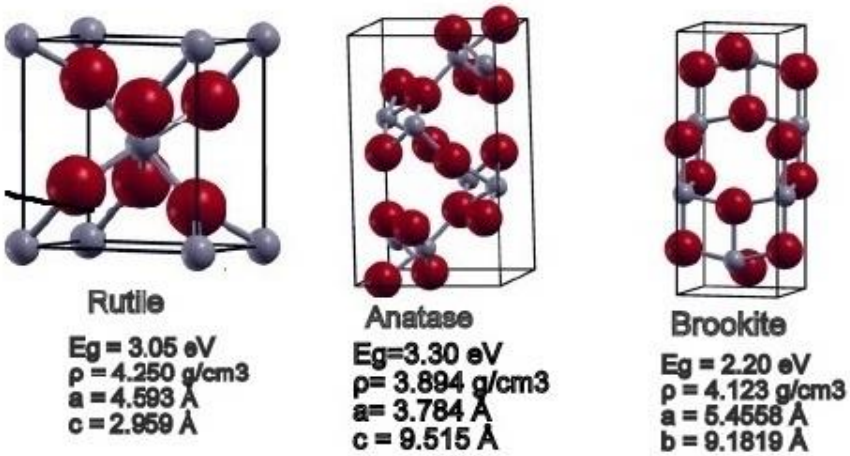

Figure 1.1. Morphological forms of TiO_2.

1.2.2 Catalytic properties and doping

As TiO_2 semiconductor have high photoatalytic properties especially anatase is very efficient for photo-degradation studies. TiO_2 is UV active but optical response of TiO_2 can be altered by changing its band gap. Band gap reduction leads to the absorption of visible radiations instead of UV light so that catalyst can easily degrade organic pollutants in the presence of visible light [22]. One efficient method of reducing ban gap is by doping. Doping intentionaly add impurities to a intrinsic semiconductor for altering its electrical, optical and other properties. After doping the semiconductor would be called as extrinsic semiconductor. In TiO_2 doping can be done by replacing Ti^{4+} by cation or by replacing O^{2-} with anion. However the former one is quite easy and common by introducing dopant into interstial spaces of crystal system. Basic conditions that are required for doping are that 1) no distortion occur 2) dopant should be more than 1% 3) size and ionic radius of dopant should be same as the size or ionic radius of atom of crystal. TiO_2 has been doped by different metal ions, noble matals, metalloids, non-metal ions by making composites, co-doping, doping, hybridization, coupling and capping [23].

1.2.3 Mechanism of TiO_2 action

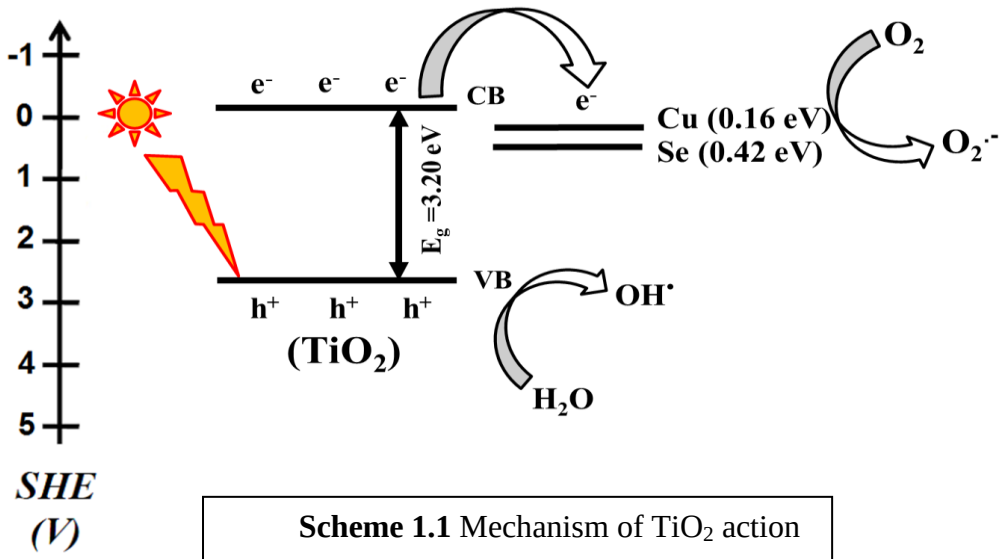

Scheme 1.1 Mechanism of TiO_2 action

TiO_2 anatase has band gap of 3.20 Ev. Its valence band is at 2.9 eV and conduction band is at -0.34eV in NHE. The bands of dopants i.e copper in form of Cu^{+2} lies below the conduction band of TiO_2 having value of 0.16 eV in NHE while the band gap of selenium in form of Se^{+2} lies below the CB of TiO_2 at position 0.42 eV. So when light of same or higher wavelength than the energy gap between VB and CB of semiconductor get excited and move

to the conduction band forming holes in valence band electrons instead of coming back to VB get trapped into the impurity (dopant) band introduced below CB hence decreasing the electron-hole recombination rate. The electrons in the CB can reduce O_2 into $O_2^{\cdot-}$ and holes in the valence band react with surface absorbed H_2O or OH^- results in the formation of hydroxyl radicals ($OH^{\cdot}$), hydrogen peroxide (H_2O_2) and protonated superoxide radical ($HOO^{\cdot}$) [24-26]

1.3 Pesticides

Pesticides are chemical substances that are used against pests and other organisms that cause harm to plants and animals. They may kill or deters pest. Pesticide is vast term and it includes fungicide, nematicide, herbicide, antimicrobial, animal repellent, rodenticide, bactericide, disinfectant, insect growth regulator, molluscicide, avicide, termiticide, piscicide and sanitizer. 80% of pesticides are herbicides which mostly fight against weeds, fungi, herbs and insects. Pesticide concept was introduced around 1000 b.c.e. Sulfur was used by homer to fumigate homes and in 900 c.e arsenic was used on garden pests by Chinese. During world war II some inorganic compounds like thiram, mercury, lime–sulfur, lead arsenate, copper sulfate, calcium arsenate, nicotine, selenium compounds and derris were used after World War II they were so commonly used that almost 25% of accounts has in their pockets [27].

A pesticide contains both active and inactive (inert) ingredients both have very important role. Active ingredients as indicated from name are those which destroys pest and must be mentioned on pesticide packing with its weight % while inert ingredients help in better performance of active ingredients by acting as solvent, extending shelf life of pesticide, protect pesticide from degrading in sunlight and provide safety to application. They are common food materials like edible oils, herbs and some spices. Inert ingredients actually bind all the chemicals together to form an effective pesticide and they are not necessarily nontoxic so they should be approved by EPA before use [28].

Pesticides can be classified according to their chemical nature into organic and inorganic compounds which further are classified into subclasses. Classification of pesticides are given in the **scheme 1.2.**

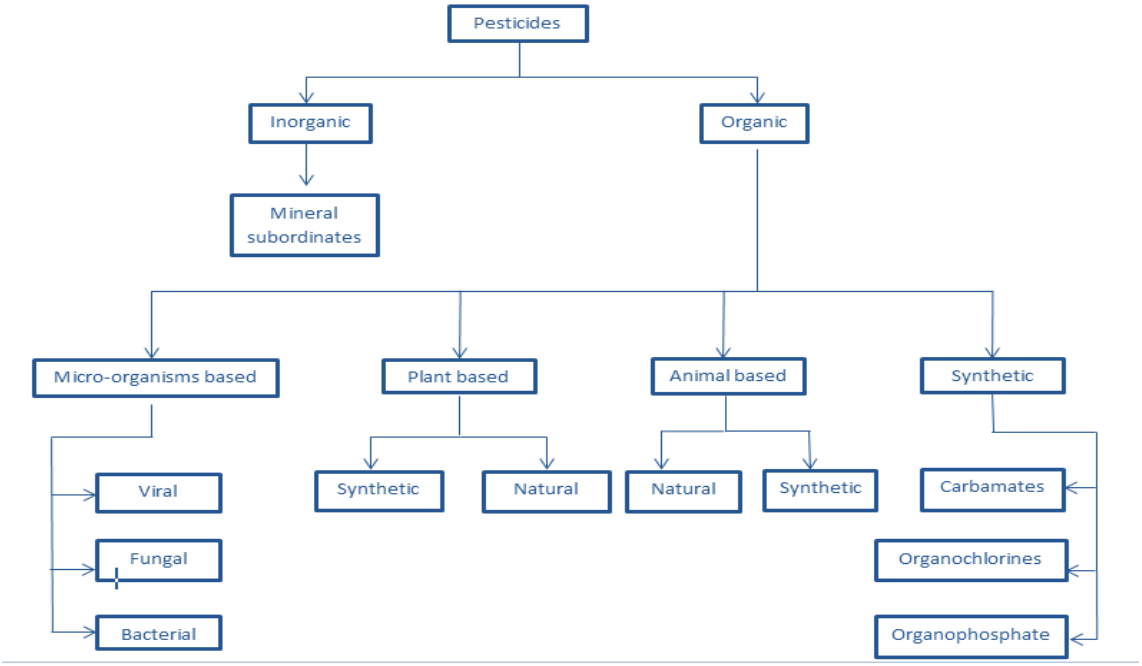

Scheme 1.2 Classification of Pesticides

1.3.1 Inorganic pesticides

Some minerals that are mined from earth can be used as inorganic pesticides by acting as poison or by inhibiting the pest action. Some examples are borates, silicates and sulfur [29].

1.3.2 Organic pesticides

Organic pesticides includes synthetic, animal based, plant based and microorganisms based. Naturally occurring pesticides have low toxicity then synthetic pesticides but this trend doesn't apply to all the organic pesticides. Organic pesticides are further divided into following classes.

1.3.3 Organophosphates

They are used in many insecticides, nerve agents and herbicides and they are generally named as esters of phosphoric acid having broad range of pests control being highly toxic class of synthetic organic pesticides [30]. They are used as fumigants and contact poison by attacking the nervous system or sometimes gastro intestinal system. Some of them are very toxic and considered as major threat to be used as pesticides while some compounds are less toxic, easily biodegradable and cause less environmental pollution. Examples are ethion, chlorpyrifos, malathion and Disulfon. Its subgroups are derived from phosphoric acid like organo-thiophosphates [31].

1.3.4 Carbamates

Very similar to ops in structure but derived from carbamic acid as organophosphates are derived from phosphoric acid. They are mostly used against insect pests, against bee and wasps. They are highly poisonous and pose threats to human and animal life but don't stay in environment for very long time. Carbamates, thiocarbamates and dithiocarbamates are the subclasses of it [32].

1.3.5 Pyrethrum

Its an organic insecticide having almost 30 species. The active ingredient pyrethrins extracted from grinding of flowers of these species. Prethrin I, pyrethrin II, cinerins and jasmolins are main components. Pyrethrins containing pesticides attack on nervous system of pests. They are less toxic for mammals and birds but very toxic for fishes, considering their toxicity they are safe to be used near food items. They are used along with synergist named as piperonyl butoxide (PBO) in rural and urban areas. Synergist is not toxic themselves but play an important role in increasing the toxicity of pesticide with which they are mixed so same amount of pyrethrins would kill the pest if synergist is mixed and if not mixed the insect might recover. Pyrethrins can be synthesized which are more toxic to animals, birds and insects than natural ones. Most common examples of synthetic Pyrethrins are permethrin and allethrin [33].

1.3.6 Biopesticides/ microbial pesticides

These are certain types of pesticides that are originated from living organisms like bacteria, fungi, nematodes and plants. Their mood of action includes either by causing infection or by spreading toxicity. Example includes Bacillus sphaericus and BTI bacteria which shows activity against mosquito larvae and efficient in killing black fly larvae respectively. Biopesticides have advantage that they are economical, environmental friendly and contain no harmful residues [34].

1.4 Glyphosate

Glyphosate belongs to a class of organophosphate herbicide. It is used against annual broadleaf weeds and grasses that compete with desired crops. This herbicide was discovered by john E Franz under Monsanto company in 1970. Brought in market with trade name of

roundup. It was most commonly used herbicide in 2007 and by 2016 its use was increased by 100-fold. Some of its properties are given in **table 1.2.**

Table 1.2 Physical and chemical properties of glyphosate [35]

Chemical formula	$C_3H_8NO_5P$
Structure	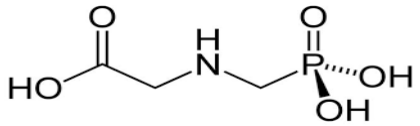
IUPAC names	N-(phosphonomethyl)glycine 2-[(phosphonomethyl)amino)acetic acid
Molar mass	169.07g/mol
Appearance	White crystalline powder
Density	1.704 at 20°C
Boiling point	187°C
Melting point	184.5°C
Solubility in water	1.01 g/100 ml
Flash point	Non-flammable

1.4.1 Mechanism of glyphosate action on living organisms

Glyphosate act by stopping the certain enzyme (shikimate kinase) pathway known as shikimic pathway and inhibits the production of certain proteins. This pathway is seven step process commonly used by algae, fungi and bacteria. This protein only produces in plants because of presence of amino acids so animals take that protein from plants [36].

1.4.2 Products of glyphosate degradation

Literature shows the degradation of glyphosate occurs from -N- bond as shown in **scheme 1.2.** Its evidence found in UV-vis spectroscopy. As -N- bond show absorbance between 200-210 nm. Degradation of glyphosate readily produce AMP (Aminomethylphosphoric acid) which further degraded into phosphoric acid. Breakdown of phosphoric acid gives inorganic phosphates [37].

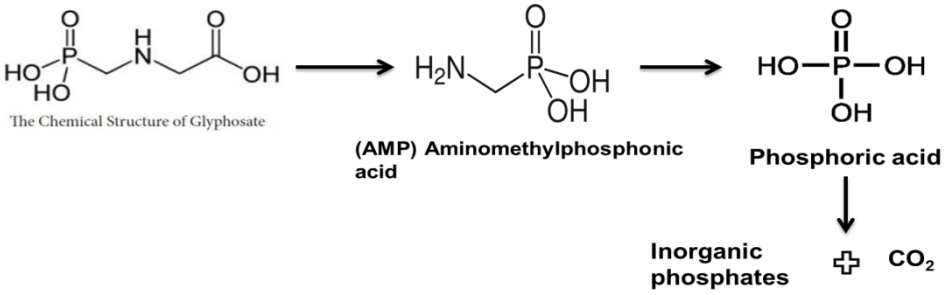

Scheme 1.3 degradation products of glyphosate [38]

1.4.3 Effect of environment

Glyphosate absorbs through roots, foliage and them strongly absorbs in soil. Afterwards moving into water bodies effect aquatic life. Half-life on glyphosate in soil is 197 days and field half-life is 47 days but half-life is highly dependent on climate and soil conditions. Median half-life in water is from few to 91 days. So it is highly recommended to degrade it without producing any harmful effects to environment [39].

1.4.4 Controversies about glyphosate

It is a world's largest herbicide to be used in terms of volume. Some studies show that people who are working with or close to this herbicide have greater risks of non-hodgkin lamphomas type cancer. Some evidences show the result of glyphosate exposure on roots and mice was carcinogenic and in human they cause some damages to DNA level [40]. But Monsanto company which is largest producer of this herbicide constantly denying these studies. So it is yet not confirm whether it cause cancer or not but some European countries banned this pesticide [41].

1.5 Dyes

Any coloured ionising or aromatic compound that are insoluble in water and attached to substrate giving it colour. Dyes have conjugated system, resonance, delocalized electrons and have at least one chromophore. Dyes absorb particular wavelength and gives colour. Also a compound called chromophore is attached to them that do some changes in energy level of dye, delocalising the electrons that give colour to dye [42]. Dyes are very vast organic compounds so they are classified into different subgroups as shown in **scheme 1.4.**

Classification: dyes are classified as

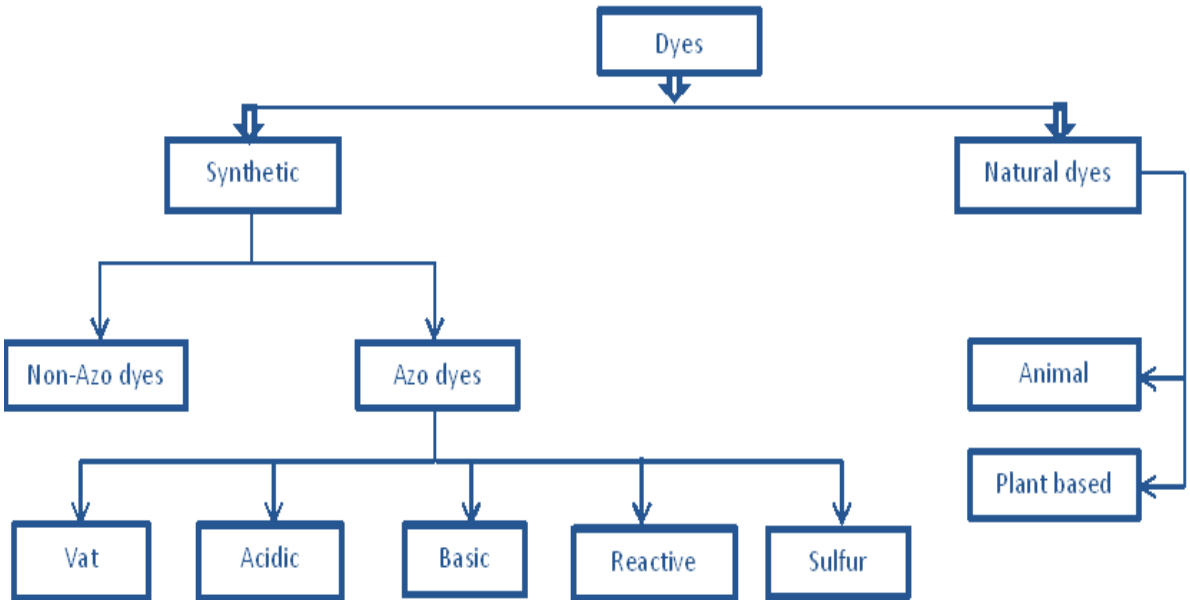

Scheme 1.4 Classification of Dyes

1.5.1 Natural dyes

Are obtained from animals, plants and minerals e.g. indigo, cochineal and ocher [43]. Some natural dyes can simply be adsorbed on the substrate surface but some requires mordant which is a chemical substance that initiates a chemical reaction between dye and fibre substrate need to be coloured. Some natural dyes are maddar that comes from roots of maddar plant. In middle ages people use natural dyes that comes from wood. Some earth minerals like limonite and hematite also give colour and can be used as dyes [44].

1.5.2 Synthetic dyes

Manmade dyes mostly formed from mineral ores or petroleum products. First discovered by William H Perkin who was British chemist in 1856 and given a name “mauve”. Examples of synthetic dyes are alizarine, triphenykmethane, arobenzen and xanthene.

1.5.3 Methyl orange

Methyl orange dye can also be used as indicator. It shows yellow colour in basic and red colour in acidic medium. Some of methyl orange properties are shown in table below

Table 1.3 Physical and chemical properties of methyl orange [45]

Common name	Methyl orange
IUPAC name	Sodium 4-{[4-dimethylamino] phenyl] diazenyl}benzene-1-sulfonate
Structure	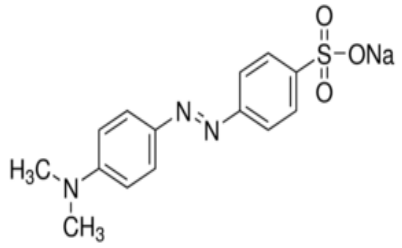
Chemical formula	$C_{14}H_{14}N_3NaO_3S$
CAS number	547-58-0
Molar mass	327.33 g/mol
Density	1.28 g/cm^3
Solubuity	Soluble in water
Metling point	>300 °C

1.5.4 Degradation products of methyl orange

Methyl orange degradation occur from azo bond as shown in **scheme 1.5**. Both side bezene rings are involved in resonsce hence N=N is available for reaction. Methyl orange degrade to form N, N- dimethyl-p-phenylenediamine which further degrade to form N, N-dimethylbenzeneamine and sulfanilic acid.

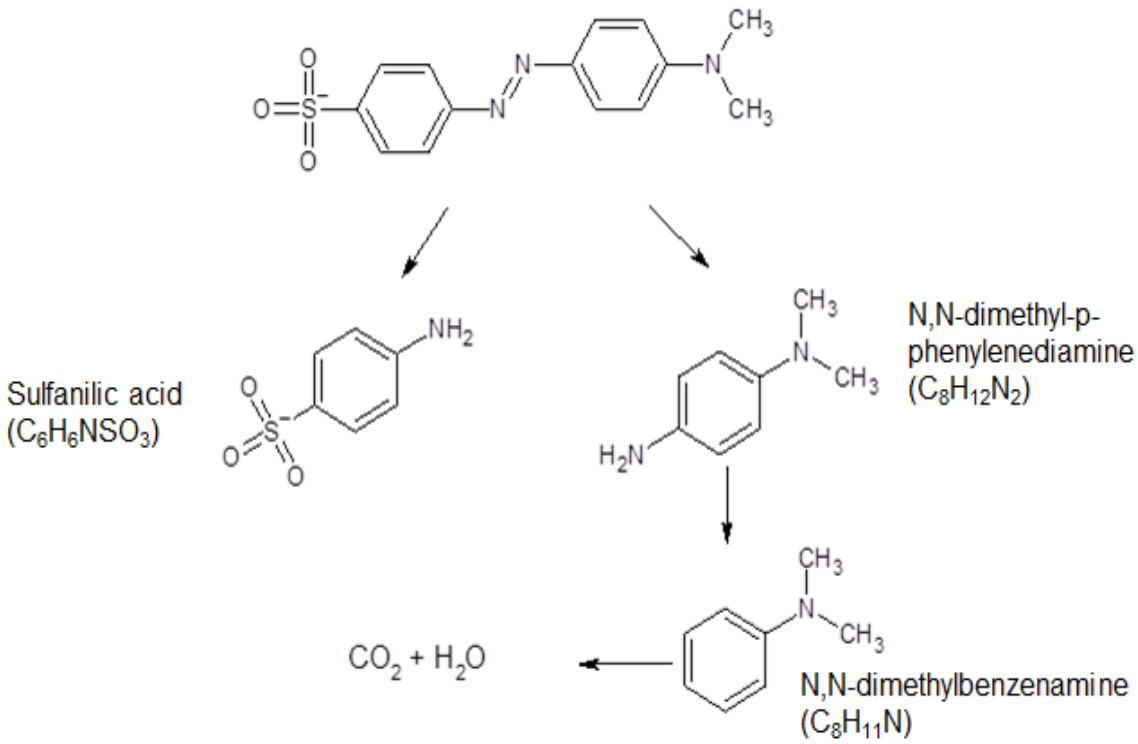

Scheme 1.5 degradation products of methyl orange [46]

1.5.5 Objectives of my research work

1. To prepare TiO_2 nanocatalyst with pure anatase phase
2. To prepare Cu doped TiO_2 with 1%, 3%, 5%, 7% and 10% dopant ratio.
3. To prepare Se doped TiO_2 with 1%, 3%, 5%, 7% and 10% dopant ratio.
4. Characterize with different techniques i.e XRD, SEM, BET and UV-Vis spectroscopy
5. To check degradation rate of Cu doped TiO_2 with methyl orange and glyphosate
6. To check degradation rate of Se doped TiO_2 with methyl orange and glyphosate

Chapter 2: Literature Review

2.1 TiO_2 as photocatalyst

Min Liu *et al.* prepared TiO_2 doped with Ti^{3+} from mixture of TiO_2 and Ti_2O_3 using facile one step thermal oxidation. Photo catalytic activity was studied using 2-propanol. Self doped TiO_2 was inactive photo chemically so it was grafted by amorphous Cu(II) oxide. Cu(II) grafted TiO_2 was efficient visible light absorber having quantum efficiency of 10.8%. grafted TiO_2 act as co-catalyst to reduce oxygen, generating photo induced electrons increasing photo catalytic activity [47].

Chrysanthi Berberidou *et al.* used commercial TiO_2 P25 semiconductor for photocatalytic degradation and mineralization studies of bentazon herbicide. Photocatalyst was loaded up to 0.5 g L^{-1}. Degradation rates were strongly affected by pH, catalyst loading, type of photocatalyst used and addition of H_2O_2. The reaction shows pseudo first order kinetics. Initial degradation rate was decreased due to H_2O_2 addition but if adding 100 mg/L of H_2O_2 increased photocatalytic degradation 2 folds. Intermediate products formed are hydroxy, dimers and bentazon are found to be more toxic than parent molecule. Vibro fischeri microbacteria and plant species sorghum saccharatum are used for toxicity tests and showed increasing trend first and then decreased later. best suitable pH for bentazon degradation was 6.0 and decreased as it goes from neutral to alkaline pH. Results show that 0.5 g/L of TiO_2 P25 eliminate herbicide in 120 min using UV irradiation [48].

Augustine Chioma Affam *et al.* used TiO_2 for degradation of pesticides chlorothalonil cypermethrin and chlorpyrifos. Photo catalysis was done under UV light. Initial concentration was varied from 0.5-2.5 g L^{-1}. COD and TOC removal were checked illustrate that H_2O_2 addition improve COD from 25.9% to 53.6% and TOC removal from 8.45% to 21.54%. While biodegradability was also improved to 0.26. Reaction followed pseudo first order kinetics and rate constant was 0.0025 for COD and 0.0008 min^{-1} for TOC removal. FT-IR showed starching vibration of carbonyl functional group (either aldehyde or carboxylic acids) at 1650.95 cm^{-1}.The band at 1519.80 cm^{-1} show C=C stretching. Band at 970.13 cm^{-1} show P=S stretching. Results showed that ammonia nitrogen was decreased from

22 to 7.8 mg/L and nitrate nitrogen was increased from 0.7 to 13.8 mg/L in first 300 min hence complete degradation of pesticide was occurred in 30 min [49].

Murtaza Sayed *et al.* investigated effect of various hydrothermal conditions like temperature, pH of solution and time of calcination. The sample prepared using hydrothermal method was TiO_2 immobilized on Ti film on various pH like 2.62, 3.04, 3.75, 4.52, and 5.38. Degradation study was done by norfloxacin in aqueous medium. Catalyst was characterized by field emission scanning electron microscopy, X-ray photoelectron spectroscopy, X-ray diffraction and high resolution transmission electron microscopy. As prepared sample has 001 faceted TiO_2/Ti with Maximum activity at pH 2.62. Particle size was determined to be 1.7 mm having sheet life morphology. Degradation intermediates and final products were studied by (UPLC-MS/MS) ultra-performance liquid chromatography tendem-mass spectroscopy. Toxicity tests were done to determine the impact of catalyst and norfloxacin on life growing and living in water. E.coli bacteria were used for toxicity tests. Cations and anions in water effect the degradation of norfloxacin while presence of H• increases and O_2 decreases the degradation and final products were less toxic than norfloxacin [50].

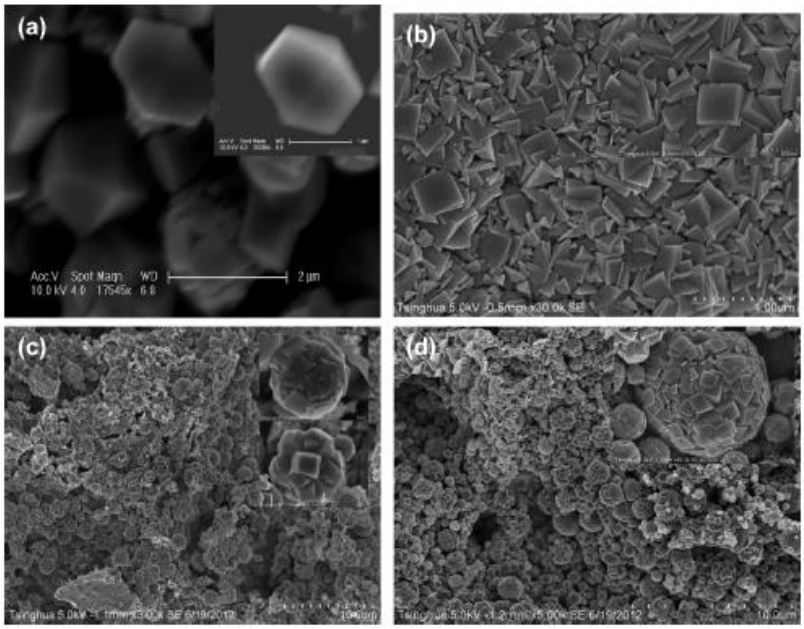

Figure 2.1. FESEM image of 001 facet TiO_2 with a) 0.01M, b) 0.02M, c) 0.03M, d) 0.04M HF concentration.

2.2 Photocatalytic studies of doped TiO_2

Jina Choi *et al.* prepared TiO^2 doped with 13 different metal ions (Ag^+, Rb^+, Ni^{2+}, Co^{2+}, Cu^{2+}, V^{3+}, Ru^{3+}, Fe^{3+}, Os^{3+}, Y^{3+}, La^{3+}, Pt^{4+}, Pt^{2+}, Cr^{3+}, Cr^{6+}) having dopants ratio ranging from 0.1- 1.0 at% using sol-gel method. Samples were characterized by XRD, SEM, BET and UV-Vis DRS. Results show that metal ions are doped by directly substituting Ti^{4+} ions or by incorporating itself into interstitial positions based on their ionic sizes. Highest photo catalytic activity was shown by Pt^{4+} and Pt^{2+} using methylene blue. Doping with Pt, Cr, V, Fe, Rb lower the anatase to rutile transformation temperature. There is no relation between valance state or ionic size and anatase to rutile transformation [51].

2.3 Metal doping

M.B. Suwarnkar *et al.* prepared samples with different Ag content from 0.12 to 0.5 mol% by microwave assisted method. This method is energy efficient, control particle size and gives short reaction time. Doping gives pseudo cube like morphology. Crystallite size for pristine TiO_2 is 15 nm and is decreased on doping up to 10 nm for 0.25 mol%. Photocatalytic activity was studied on methyl orange by varying the amount of catalyst from 0.6 to 1.4 g/dm^3. Highest activity was shown by 0.25 mol% doping. Catalyst's surface charge and pH are parameters effecting photocatalytic activity[52].

S. Y. Mendiola-Alvarez *et al.* synthesized semiconductor material Cr(III) doped TiO_2 by microwave assisted sol-gel method with different doping concentrations of 0.02, 0.04 and 0.06 wt%. This method was chosen because of its various advantages of high reaction rates, shorter reaction time, phase purity and rapid heating. Characterization was done by XRD, SEM, UV-Vis DRS, nitrogen physisorption and AAS. Photo catalytic studies were done using MCPA (4-chloro-2-methylphenoxyacetic acid) followed by HPLC and TOC analysis. Doped catalysts have large surface area, small crystalline size and have mesoporous structure having pore diameters ranging from 5.6-6.5 mm. 0.04% Cr(III) doped TiO_2 have shown more activity than bare TiO_2. Activity of catalyst mainly depends upon amount of doping agent, synthesis procedure and nature of dopant. Results showed that crystallite size decreased from 20 to 4 nm as dopant amount increased and intermediates formed were (HBDM) and 2- hydroxybuta-1,3-diene-1,4-diyl-bis (oxy)dimethanol, (CMP) 4-chloro-2-methylphenol, (HMPA) 2-(4-hydroxy-2-methylphenoxy) acetic acid. Photocatalytic activity

was studied using both visible and UV light at pH 3.5. CMP is more toxic than MCPA but completely removed in 180 min using 0.04% CrTi catalyst [53].

J. Choina *et al.* prepared Zr doped TiO_2 using chemical vapor deposition and sol-gel method. Characterization was done by SEM, XRD and TEM. Intermediates were examined using UV-Vis spectroscopy, HPLC and GC/MS by decomposition a pharmaceutical compound called ibuprofen. Results show an improved yield using chemical vapor deposition and sol-gel method. Zr doped TiO_2 show improved degradation as compared to simple titania with less amount of catalyst used. Catalyst shows mesoporosity while intermediates and some polymeric compounds formed lead to faster deactivation of catalyst because of their toxicity [54].

Rongfang Yuana *et al.* synthesized Fe doped, Al doped and codoped TiO_2 to use it against humic acid under UV irradiations. catalysts were prepared through hydrothermal method and calcine at 550°C. Al^{3+} and Fe^{3+} occupy the interstitial spaces in TiO_2. SEM showed that doped catalyst had nanotubes morphology. Reaction follows pseudo first order mechanism and rate constant was 0.172 min^{-1}. Results showed that doped catalyst degrade 79.4% of humic acid. Co doped TiO_2 had more efficiency than other catalysts [55].

Arghya Narayan Banerjee *et al.* synthesized Ga doped anatase TiO_2 using sol-gel method for degradation of toxic organic compounds in water under UV irradiation. Ga^{+3} (ionic radii 62 pm) can replace Ti^{+4} (ionic radii 68 pm). Ga doped TiO_2 had 97% degradation efficiency within 3 h. Reaction follow pseudo first order kinetics and rate constant was 1.3×10^{-2} min^{-1}. Particle size was 15 nm [56].

2.4 Non-metal doping

A.N. Kadam *et al.* prepared nitrogen doped TiO_2 using microwave assisted method with ammonia as hydrolyzing agent. catalyst are characterized by XRD which shows their crystallite size ranging from 10-15 nm. SEM shows that they possess pseudo spherical shape. FT-IR gives bands at 2923-2825 cm^{-1} are C-H stretching and at 670-735 cm^{-1} the broad peak of Ti-O bending. TGA-DTA shows that there are three weight losses occur. To check maximum degradation efficiency effect of pH, light sources and effect of catalyst loading are taken into account. Doping resulted in ten times increased degradation rate of malathion. Increasing temperature of calcination increased crystallinity. As pH was increased the degradation activity becomes high and maximum activity 97% was reported at pH 6 but

further increasing pH decreased the activity. Under UV light using 1 g/dm^3 of N-doped TiO_2 with 5 ppm malathion at pH 6, 97% of malathion is degraded in 150 min and COD was reduced from 50 to 10 mg/dm^3[57].

Rahmatollah Rahimi *et al.* prepared N-S doped TiO_2 in anatase phase using sol-gel method for degradation of 4-nitrophenol. Precursor used were TTIP, Titanium tetrachloride, ammonium Sulfate $(NH_4)_2$ SO_4. Sol was stirred for 24 h and calcined for 4 h at 600°C and 800°C. Characterization was done by XRD, EDAX, FT-IR, DRS and SEM. Results showed that pH 6 was suitable for effective degradation. Comparison of commercial TiO_2 P25, prepared TiO_2 and N-S doped TiO_2 was made which showed that N-S doped TiO_2 had highest photocatalytic activity. Band gap of TiO_2 P25 was more. Doping lower the band gap significantly. Maximum activity was shown by N-S doped TiO_2 calcined at 800°C this was because TiO_2 prepared by titanium tetrachloride was agglomerated. After washing with ethanol this sample doesn't show improvement while TiO_2 prepared by TTIP don't need washing at all. FT-IR results showed stretching vibration of OH group and Ti-O at 500 cm^{-1}. Ti-O-S peak appeared at 1050 cm^{-1}. Ti-O-N peak appeared at 1100 cm^{-1} [58].

Kavitha Pathakoti *et al.* used sulfur doped TiO_2, nitrogen-fluorine codoped TiO_2 and TiO_2 for degradataion of organic compounds under visible light. Catalysts were prepared by sol-gel method. Photo deactivation was investigated by E.coli. For E.coli best results were shown by commercial TiO_2 P25. S-doped TiO_2 was slightly toxic may be because of their small size (3.8 nm) thermally unstable and high specific surface area while TiO_2 NPs and N-F TiO_2 had no effect on bacteria. Particle size and surface area significantly affect biological and chemical activity. Particle size <100 nm decreases biological and chemical activity while <10 nm increases the activity. So it was demonstrated that size and surface area affects activity largely [59].

Akbar Eslami *et al.* prepared nitrogen and sulfur co-doped TiO_2 nanosheets and nanoparticles using sol-gel and hydrothermal method and used them for photocatalytic degradation of anti-inflammatory and non-steroidal drugs known as NPX (naproxen) and IBP (ibuprofen) under sun light. Catalyst contain 72% of anatase and 28% of rutile. SEM and TEM showed morphology and particle size. Nanoparticles were mesoporous having both rutile and anatase phase. TEM showed homogenous spheroid morphology and particle size of 5-10 nm of nanoparticles but nanosheets were of 20-25 nm length. Surface area determined by BET was 132 m^2/g for nanoparticles and 64 m^2/g for nanosheets. It was clear from results

that 2.0 g/L. N,S-TiO_2 nanoparticles can degrade 99.3% and 85% of NPX and IBP. N,S-TiO_2 can be reused 6 times efficiently [60].

Le Dien Than *et al.* prepared N doped TiO_2 nanoparticles using sol-gel method. Degradation studies were done using methylene blue under visible light irradiation. Catalyst was calcine at different temperatures like 500, 600, 700 and 800°C. Results showed that increasing calcination temperature decreases particles size and increases surface area which leads to better photo catalytic activity. Increasing calcination temperature increases the conversion of rutile to anatase phase [61].

M. Antonopoulou *et al.* prepared N doped, N,S co doped TiO_2 by sol-gel. Characterization was done by XRD, SEM, BET, UV-Vis spectroscopy and TGA-DTA. Degradation activity was determined by Tris (1-chloro-2-propyl) phosphate (TCPP) an organophosphorous flame retardant. Doping increased surface area and mesoporous crystalline anatase.N,S codoped TiO_2 showed better activity under visible light at pH 6 [62].

2.5 Nano-Composite studies

A.Perez –larios *et al.* synthesized ZnO-TiO_2 composite with different ratio of 1.0, 3.0, 5.0 and 10.0 wt.% Zn by sol-gel method and used for hydrogen production. For ZnO precursor used was $Zn(NO_3)$-$6H_2O$. Catalyst was characterized by XRD, SEM, XPS, EDS, nitrogen physisorption and Raman. Specific surface area was ranging from 85-159 m^2/g. XRD result showed that anatase phase is dominant. Due to ZnO doping band gap was reduced from 3.05 to 3.12 eV. Water splitting of this ZnO/TiO_2 catalyst was 1300 mol/h which is six times more than ordinary TiO_2. Pyrex reactor was used to check photo catalytic activity which has water-ethanol and 0.1g catalyst. Hg lamp was used for irradiation. Crystallite size was ranging from 7.2-5.7 nm. Raman spectroscopy showed bands at 640, 513, 395 and 145 cm^{-1}. ZnO had a positive effect on hydrogen production [63].

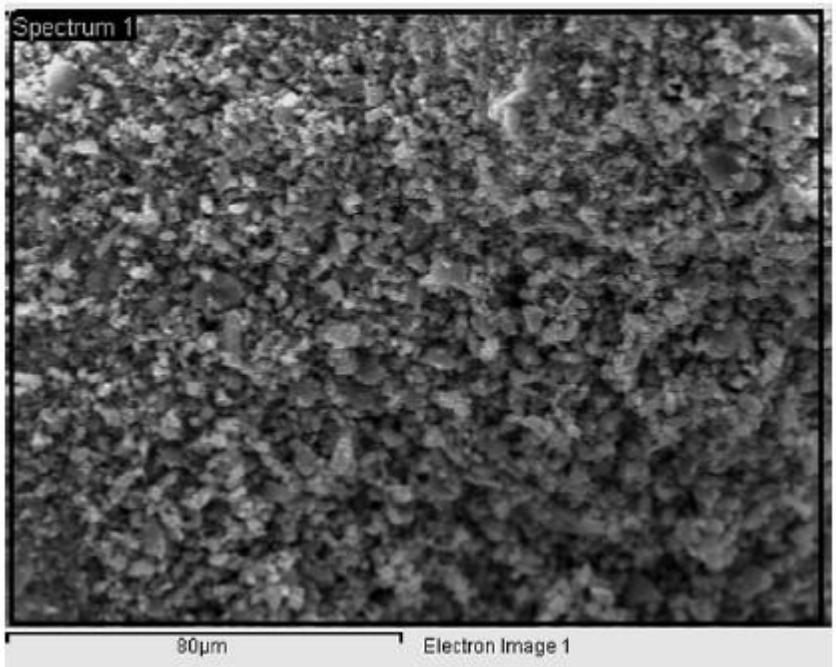

Figure 2.2. SEM image of 1.0wt.% of ZnO.

Hiwa Hossaini *et al.* prepared TiO_2 doped with N, NS, FeNS and FeFNS for degradation of pesticide diazion. Preparation of catalyst was done by sol-gel method. Precursor used for TiO_2 was titanium(IV) n-butoxide, thiourea and trifluoroacetic acid . N doped TiO_2 was prepared by hydrothermal method. Characterization was done by XRD,SEM, UV-Vis spectroscopy. Highest photocatalytic activity was found to be of FeFNS doped TiO_2 which is mesoporous having crystallite size of 6.7 nm, surface area of 104.4 m^2/g and pore diameter of 10.2 nm. At pH 7 over 52.3% of diazinon was degraded in 100 min. Reaction kinetics was pseudo first order. Material was found in both anatase and rutile phase and about 87% of material was rutile phase. 26.3, 13.6, 14.3, 6.2, 10.9, and 6.7 nm were crystallite sizes for of commercial TiO_2, as-made TiO_2(pure TiO_2), N-TiO_2, NS-TiO_2, FeNS-TiO_2 and FeFNS-TiO_2. In dark the total amount that was absorbed by onto commercial TiO_2, as-made TiO_2, N-doped TiO_2, NS-doped TiO_2, FeNS-doped TiO_2, and FeFNS-TiO_2 was was 8.3%, 12.4%, 17%, 15%, 12%, and 35% respectively. FeFNS/TiO_2 follows pseudo first order with rate constants of 0.973 h^{-1} and 0.581 h^{-1} [64].

M. A. Barakat *et al.* investigated degradation efficiency of methomy pesticides by preparing a composite of $CdSO_4/TiO_2$ by sol-gel method. Grinding drying and calcination of sample reduced its particle size. $CdSO_4$ form schottky defects which capture electrons and enhanced the degradation rate or dipole nature of $CdSO_4$ also enhance activity.

As prepared catalyst successfully degrade pesticide under sunlight with removal capacity of 300, 500, 1000 and 2000 mg/L in 30, 30, 40 and 60 min respectively [65].

S. Dominguez *et al.* prepared magnetic and visible light active Nano composites of TiO_2-WO_3 and used for degradation of biphenol A. Other materials were used for comparison like Fe_3O_4@SiO_2@TiO_2, TiO_2 P25 and TiO_2. SEM, HR-TEM, XRD, BET and EDS were used for characterization. Results showed a decrease in magnetic character from TiO_2, TiO_2-WO_3 and Fe_3O_4@SiO_2@TiO_2-WO_3 and values are 90%, 27.9% and 17.5% respectively. Benefit of these catalysts was that they can be separated magnetically and can be reused. Degradation efficiency was also checked using waste water which was quite remarkable. SEM and TEM showed spherical particles with diameter. Fe_3O_4@SiO_2@TiO_2-WO_3 was in core-shell form having core of Fe_3O_4 with size of 17 nm they were aggregated and in large clusters. Other layers on these particles were SiO_2 and TiO_2-WO_3 which form rings on core particles. Degradation activity of intermediates like 2-(4-hydroxyphenyl)-2-Propanol was also studied and it was reported that TiO_2 P25 has highest activity among all catalysts [66].

Yanna Tang *et al.* investigated the degradation efficiency of core-shell particles $NaYF_4$:Yb, $NaYF_4$:Yb,Tm@TiO_2 and TiO_2. TiO_2 as core and $NaYF_4$ act as shell was prepared by Stöber process. $NaYF_4$:Yb and $NaYF_4$:Yb,Tm@TiO_2 were prepared by solvothermal process and two step wet chemical method. Methylene blue was used for degradation of $NaYF_4$:Yb,Tm@TiO_2 and other catalysts under infrared irradiation. Results indicate that reactive oxygen species. $NaYF_4$:Yb,Tm@TiO_2 has more catalytic activity than other catalyst [67].

Cordero Garcia *et al.* investigated the degradation of DCF (sodium diclofenac) using nitrogen doped WO_3/TiO_2 nano composite. Sol-gel method was used for preparation having tetrabutyl orthotitanate, ammonium p-tungstate and ammonium nitrate as precursors. X-ray diffraction, transmission electron microscopy, scanning electron microscopy, UV-Vis spectroscopy, X-ray photoelectron spectroscopy. photo catalytic efficiency was measured by batch reactor results showed that 100% DCF was degraded by WO_3/TiO_2 catalyst. WO_3 has bandgap of 2.3 eV while TiO_2 has band gap of 3.2 eV so coupling both of them would decrease band gap [68].

Md Ahsan Habib *et al.* synthesized ZnO-TiO_2 nanocomposites using sol-gel for azo dye degradation. Catalysts were calcined at 600°C and 900°C to determine the effect

of temperature. As prepared samples have low band gap compared to TiO_2. Results showed that 6 g/L of ZnO-TiO_2 catalyst was able to degrade 97-98% of bright golden yellow dyes in 2 h at pH 7 under sunlight. But degradation efficiency increases as pH is increased up to pH 7 and then decreased because of zero point charge. Surface of catalysts become positive in low pH ranges and negative in pH values above 7. Reaction was pseudo first order. The average particle size determined by XRD was 500 nm and calcination temperature didn't affect particle size [69].

Mario J. *et al.* reported the synthesis of two oxides CeO_2 and TiO_2 and effect of their interface on degradation of toluene. Ceria sample were in different ranges from 1-10 mol%. Catalysts were analyzed by XRD, SEM, BET and UV-Vis spectroscopy showed that the oxide-oxide contact enhances the photo activity up to 3.5 times than simple TiO_2. Ce-Ti interface trap electrons in it hence lowering electron-hole recombination. Particle size was 12-15 nm. To understand the behavior of CeO_2-TiO_2 a new spectro-kinetic method was developed which gather data on basis of kinetics, charge carriers and interaction of catalyst with light. Relation found between elimination of toluene and available surface hole related species and that was a quasi-linear one. This was proof that oxide-oxide interface was a center of electron capturing and increasing degradation rates [70].

Jinxiu Wang *et al.* prepared nanocomposites of Ag_3VO_4/TiO_2 using cost effective coupling method. Samples were used for decomposition of benzene. Only 0.5% of sample was required for efficient degradation. Photochemical studies confirmed that doping TiO_2 with Ag_3VO_4 improved charge separation. Quartz photo reactor having 500W Xe-arc lamp was used loaded with 1 .7 g of catalyst. Catalyst was first passed through stainless steel holes to get uniform size which was 0.21-0.25 nm. Results showed that Ag_3VO_4 efficiently convert anatase to rutile and exhibit large surface area which is good for photo catalytic activity [71].

Vaclav Stengl *et al.* reported the synthesis of In^{3+} doped TiO_2 nanoparitcles and TiO_2/InS_3 nanocomposites for degrading warfare agents and water pollutants like thioacetamide and urea respectively. Crystallite size decreases with increase of dopant concentration. In^{3+} has size of 0.080 nm and Ti^{4+} has size of 0.0605 nm so it was difficult to incorporate In^{3+} but increasing its concentration would replace Ti^{4+}. Photocatalytic results showed that TiO_2 / In_2S_3 were efficient to degrade sulfur mustard up to 98.5% under visible light [72].

2.6 Photocatalytic studies of Graphene doped TiO_2

B. A. Bhanvase *et al.* reported the synthesis of graphene doped TiO_2 by hydrothermal method for waste water treatment. Particle size, surface area and morphology was determined by XRD, BET, SEM and DRS. Surface area was 2600 m^2g having nanoflower like shape. Graphene doped TiO_2 was more effective in degrading organic pollutant as compared to undoped TiO_2. FT-IR spectra showed C-H, C-C and C-S peaks. The as prepared catalysts remove 50% of pollutants from waste water in 30 min [73].

Xue Liu *et al.* reported TiO_2 reduced with graphene oxide nanocomposites by redesigned Hummers method for degradation of triazine, chloroacetanilide and phenylurea. RGO was doped in 2, 5, 10, 30 and 100 wt% . Best results were found to be with 2% doped TiO_2/GO. TiO_2 efficiency was increased so this method was reported as an efficient route to prepare catalysts. Results showed that these herbicides were removed irradiating with sunlight within 5 h. Bands at 458.41, 464.5 and 458.9 eV shows that Ti2p, Ti $2p_{1/2}$ and $2p_{3/2}$ binding energies are present. Peak intensities of peaks at 286.9 and 288.8 eV are reduced significantly which depict that GO was reduced [74].

Nailiang Yang *et al.* prepared graphene doped TiO_2 composites, carbon supported TiO_2 and TiO_2-graphdiyne by hydrothermal process. Results showed that TiO_2-graphdiyne show better oxidation and charge separation compared to other catalysts so it was best catalyst for degradation of methylene blue. Rate constant of reaction was 1.63 for TiO_2-graphdiyne and reaction has first order kinetics [75].

2.7 Doping of lanthanide elements

Khalid Umar *et al.* used hydrothermal process for synthesis Mn, Ce and La doped TiO_2 with concentration difference of 0.15%, 0.30%, 0.45%, 0.60%.Synthesis was done by using titanium tetrachloride, manganese (II) sulfate monohydrate as precursors. Characterization was done by XRS, SEM, TEM, UV-Vis spectroscopy. Ionic radii of Mn and La were 0.080 Å and 0.1016 Å respectively, so it's very difficult for these ions to penetrate into interstitial sites rather they are present on surface layer of TiO_2 confirmed by SEM and TEM. Structural morphology was found to be irregular, porous and rather rough surface. Results showed that catalyst with dopant ratio of 0.45% decreased the recombination rate. Maximum Photo catalytic activity was observed for 0.45% Mn doped TiO_2. For degradation studies 0.35 mM glyphosate and 0.50 mM methylene blue was used and 50% of their amount

was converted into less harmful molecules using 0.45% Mn doped TiO_2 in 300 min irradiation time [76].

Vignesh C *et al.* reported TiO_2 pure anatase doped with Er and Yb ions by hydrothermal method for degradation of phenol studied in sunlight. Dopant concentration was 0, 2, 10, 15 and 20%. Reaction followed pseudo first order kinetics. Ions were incorporated into TiO2 phase. Photocataltyic degradation studies were done by reactor having high intensity LED lamp. Results showed that 2% of Er and 10% of Yb was best for degradation. Along with phenol a comment pollutant also used in eye drops was also degraded [77].

2.8 Pesticides degradation

M. Salazar-Villanuevaa *et al.* prepared metal doped TiO_2 by colloidal method. Metals used for doping are Zn, Ga and Ge with 1% in wt. calcination was done at 400°C to get purely anatase phase. Characterization was done by XRD, SEM, UV-Vis spectroscopy, XPS and DRS. XPS showed presence of doped entity in catalyst. It also showed some energy levels like $2p_{3/2}$ and $2p_{1/2}$ which are from doping materials. 2,4 dichlorophenoxyacetic acid mixed in water was used for catalytic studies. Photocatalytic studies showed that decreasing order of degradation was Ge: TiO_2 > Ga: TiO_2 > Zn: TiO_2 > TiO_2. Atomic radii of Ge, Ga and Zn were 53 Å, 62 Å, 74 Å respectively so they were inserted into TiO_2 matrix. Particle size was 0.62, 0.55 and 0.59 for Ge, Ga and Zn respectively. Ge doped TiO_2 showed maximum activity and 50% of hedonal was degraded in first 20 min [78].

P. Singla *et al.* prepared Ni doped and undoped TiO_2 using sol-gel method for degradation of endocrine disturbing compounds known as phthalate esters. Precursor used were TTIP (titanium(IV) isopropoxide) and nickel nitrate hexahydrate ($Ni(NO_3)_2 \cdot 6H_2O$). Ratio of $Ni^{2+/}Ti^{4+}$ varied from 0.2 to 0.6 mol%. Their mixture with ethanol and distill water was stirred for 2 hours and then aged for 1 day then dried. Powder obtained was calcined for 2 h at 450 °C. samples were characterized by XRD, SEM UV-Vis DRS, TGA, FT-IR. Particle size calculated from XRD for doped and undoped catalyst was 15 nm and 20 nm showing a decrease in particle size on doping. FT-IR showed bands of stretching vibrations of Ti-O-Ti and Ti-O at about 500 cm^{-1}. Photocatalytic activity was studied in a borosilicate glass made column photoreactor. Catalyst with Ni ratio of 0.6 mol% showed best

photocatlytic activity due to decreased size. SEM images show no significant change in morphology on increasing dopant concentration [79].

Taranjeet Kaur *et al.* used Fe doped TiO_2 which was prepared by surface impregnation method with different dopant ratios of 1%, 2%, 3%, 4%. Commercial TiO_2 was used and dopant precursor used was Fe_2O_3. Sol was prepared and aged for 24 h then calcine for 2 h. Catalysts were characterized by XRD, FESEM, TEM, EDS. Crystallite size was found to be 25-34 nm and band gap was reduced from 3.2 eV to 2.8 eV. Reaction followed pseudo first order kinetics. Photo catalytic efficiency was measured using propiconazole and carbendazim studied through UV spectrophotometer. Degradation was done both under sunlight and in dark. 2% ratio of dopant showed maximum degradation both in light and dark. 98.5% of carbendazim in 60 min and 92% of propiconazole in 90 min were degraded. Catalysts were irregular in shape. Mineralization was also checked by measuring COD which showed that large and complex compounds are converted into smaller molecules [80].

Javed Ali Khan *et al.* prepared phosphorous (P) and fluorine (F) doped and codoped TiO_2 by new sol-gel method for degradation of Atrazine in water. Precursor used were Titanium (IV) isopropoxide (TTIP), ammonium fluoride (NH_4F) and H_3PO_4. Characterization was done by UV-Vis DRS, XRD, FT-IR, HR-TEM, XPS and Raman spectroscopy. Catalysts prepared had high surface area, mesoporous with pore diameter ranging from 4.0-2.5 nm and decreased band gap of 2.70 eV. Surface area determined by BET were 79.7, 175.0, 88.8 and 212.0 m^2/g of simple TiO_2, P doped TiO_2, F doped TiO_2 and PF codoped TiO_2. FT-IR showed stretching vibration at 3420 cm^{-1} attributed to hydroxyl groups, a peak at 1640 cm^{-1} was of absorbed surface water. More absorption of water molecules results in better photo catalytic activity. 1045 cm^{-1} peak was due to Ti-O-P vibrations. Particle size was calculated by Scherrer formula was 19.9 nm, 17.8 nm, 9.1 nm and 7.4 nm for simple TiO_2, F-TiO_2, P-TiO_2 and PF-TiO_2 respectively [81].

Romina Zabar *et al.* degraded three pesticides clothianidin, imidacloprid and thiamethoxam using TiO_2 immobilised on glass slide. Reactor used consists of six polychromatic fluorescent UV working at 355 nm. Mineralization of three pesticides showed that imidacloprid, thiamethoxam and clothianidin had 0.2%, 2.9% and 0.4% respectively. Several intermediates were formed which were observed using HPLC-DAD (High Performance Liquid Chromatography with Diode-Array Detection) analyses. Within 2 h of irradiation by low pressure mercury lamp the pesticides were removed up to 0.1%, 2.0% and

0.01% of imidacloprid, thiamethoxam and clothianidin respectively. All three pesticides show first order decay [82].

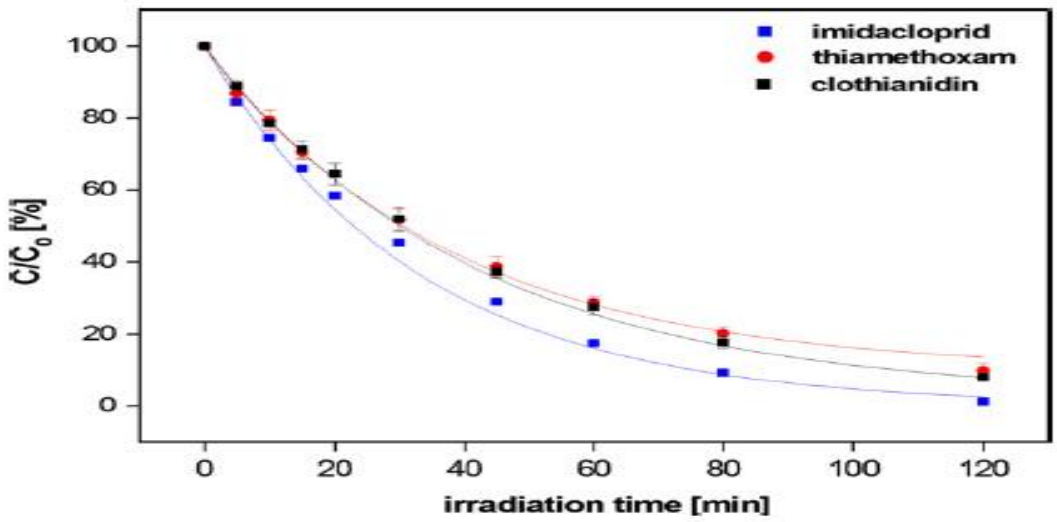

Figure 2.3. Degradation curves of imidacloprid, thiamethoxan and clothianidin with respect to time.

Said M. El-Sheikh *et al.* investigated the photo degradation of ibuprofen. They prepared nitrogen and carbon co-doped TiO_2 using one-pot hydrothermal method. XRD pattern determined the presence of mixed brookite and anatase phase having mesoporous and quasi spherical nanoparticles. Doping lowered band gap up to 2.85 eV. Complete characterization showed that 25.6% brookite and 74.4% of anatase phase. Illuminated with visible light the catalyst degrade 99% of ibuprofen. Surface area ranges from 21-65 m^2/g and particle diameter and length was 25 and 108 nm [83].

2.9 Dyes degradation

Ali Bumajdad *et al.* work was focused on preparation of mesoporous Au doped TiO_2 particles by deposition-precipitation method. For determination of particle size and other qualities XRD, ICP-OES, XPS, TEM and SEM was used. Degradation of Safranin-O was studied both in sunlight and ultraviolet irradiation. Au particles were incorporated into interparticles pores of TiO_2. 97% of dye degraded in 50 min. crystallite size was 7.1 nm for doped catalyst while undoped was slightly smaller than that also confirmed by TEM. Nobel metals restrict degradation in sunlight due to localized surface plasmon resonance that results in heat generation. Au NPs doping decrease the band gap and hence decrease time for

electron-hole recombination. So the doped catalyst becomes visible light active. Previous studies report that low surface area and less crystallite size increases the catalytic activity which was demonstrated by this work [84].

T.V.L Thejaswinia *et al.* reported degradation of acid red 85 using Bi doped TiO_2 and Bi-N codoped TiO_2 under visible light. Different quantities of Bi used for doping were 2.5, 5.0 and 10.0 wt.% after vigorous mixing samples were allowed to dry at 80°C for 24 h and calcined for 500°C for 4 h. Acid red 85 was used to investigate the influence of varying parameters like quantity of catalyst, concentration of dye, pH, time and intensity and electron acceptors. Characterization by XRD, SEM, BET, XPS, UV-Vis-DRS, TGA and TEM. Band gaps for Bi-N-TiO_2, Bi-TiO_2 and TiO_2 were 2.88, 3.01 and 3.15 eV and show more degradation with modified samples only used 20 g/L. Bi^{3+} bonded with TiO_2 and Nitrogen ions were present in interstitial spaces of TiO_2 were both confirmed by XRD and XPS. Size of particles were ranging from 36-43 nm confirmed by SEM and TEM. Surface area for Bi-TiO_2 and Bi-N-TiO_2 was 29.9 and 31.7 m^2/g respectively determined by BET. Dye was more efficiently degraded on pH 4.0 and 3.0 within 10 min of irradiation of visible light [43].

Hassan Koohestani *et al.* studied the effect of CuO/TiO_2 nanocomposites prepared with different ratios of CuO on TiO_2 for degradation of methyl orange dye. Catalysts were prepared by sol-gel method. CuO doped was 5, 7, 10 and 12.5 wt%. BET showed that surface area of composites was lower than TiO_2 and particle size was 16-19 nm. Band gap decreased from 2.95 to 2.30 eV for 5-12.5 wt% doped catalysts respectively. Catalysts were slightly spherical in shape. Photocatalytic degradation was done under UV lamp showed that from all catalyst the maximum degradation efficiency was of 7wt % CuO because further increasing the amount of dopant causes agglomeration on surface of TiO_2. This agglomeration restricts the entry of light on TiO_2 [45].

Chapter 3: Experimental work

3.1 Synthesis of TiO_2 nanoparticles

The lab work of research project started with synthesis of TiO_2 nanoparticles by simple sol-gel method.

Material: Titanium isopropoxide (Sigma Aldrich), 2-propanol (Sigma Aldrich), HCl, distilled water, $CuSO_4.5H_20$ (Sigma Aldrich), SeO_2.

Procedure: The TiO_2 nanoparticles were prepared by sol-gel method at room temperature and at acidic pH. Experiments were done by following steps;

3.2 Preparing the colloidal solution

In first step titanium (IV) isopropoxide (5 ml) was added in 2-propanol (50 ml). In another beaker 50 ml of distilled water was added and 2-3 drops of HCl was added to maintain pH of water up to 2. After that first solution of TTIP and 2-propanol was added in 2nd solution along with dopant precursor and stirred for 24 hours at room temperature as shown in **fig. 3.1** a cloudy milky solution was obtained. This solution was dried on a hot plate to remove excess solvent present and then placed in a vacuum oven at 80°C and 120 atm for 12 hours.

Figure 3.1. Stirring of Cu and Se doped TiO_2.

After drying all the catalyst in vacuum oven a solid particles more like palates were obtained. All the catalysts were ground well for 20 minutes per catalyst in a agate mortor pestle **fig 3.2 1.** Shows Cu doped TiO_2 before and after grinding and **2.** Shows Se doped TiO_2 before and after grinding. This fine powder was calcined at 500°C for 4 hours with ramp rate of 2 degree per minute.

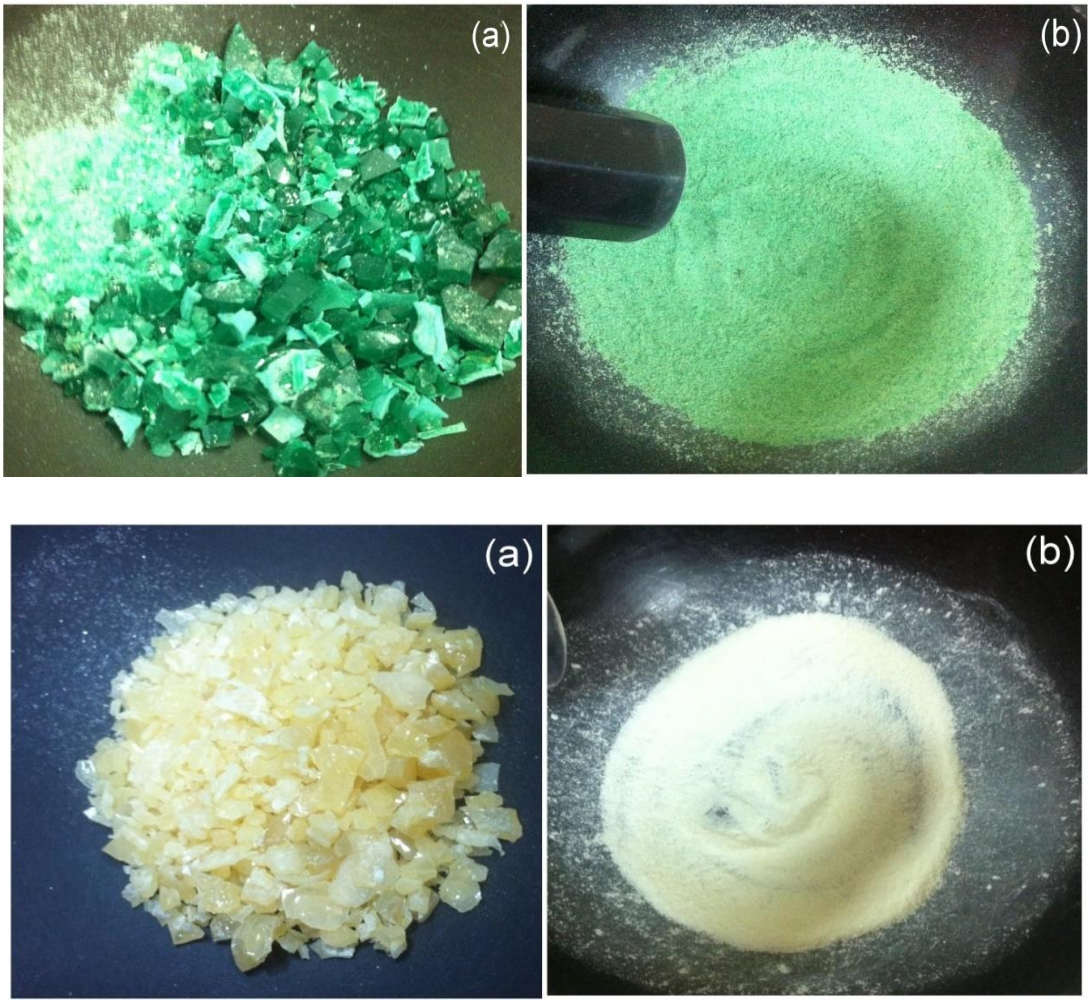

Figure 3.2.1. a) Cu doped before b) after grinding, 2. a) Se doped before b) after grinding

Table 3.1 Details of TiO_2 and dopant concentration in all nanocatalysts

Sample index	Sample composition	Calcination Temp.	Dopant percentage
TiO_2 NPs	TiO_2 nanoparticles	500°C	0%
Cu-1%	TiO_2+ Cu	500°C	1%
Cu-3%	TiO_2+ Cu	500°C	3%
Cu-5%	TiO_2+ Cu	500°C	5%
Cu-7%	TiO_2+ Cu	500°C	7%
Cu-10%	TiO_2+ Cu	500°C	10%
Se-1%	TiO_2+ Se	500°C	1%
Se-3%	TiO_2+ Se	500°C	3%
Se-5%	TiO_2+ Se	500°C	5%
Se-7%	TiO_2+ Se	500°C	7%
Se-10%	TiO_2+ Se	500°C	10%

Chapter: 4 Results and Discussion

4.1 Structural analysis

Purity and structural phase of as synthesized nano-catalysts were studied by x-ray diffraction pattern. A typical XRD pattern of Cu and Se ions doped TiO_2 nanocatalysts were synthesized by calcination at 500^0C for 4 h is shown in **fig 4.1** and **4.2**. All diffraction peaks can be assigned to tetragonal TiO_2 having pure anatase phase matched with stick pattern shown in **fig 4.3** [85].

All the results were in good agreement with the JCPDS reference card No. (00-021-1272). Impurity peaks were not observed that confirms the purity of phase. TiO_2 anatase is in highly crystalline form which can be observed from narrow and Sharpe peaks. Diffraction peaks appeared at 25.28°, 37.80°, 48.05°, 53.89°, 55.06°, 62.69°, 68.76°, 70.31° having lattice planes at (101), (004), (200), (105), (211), (204), (116) respectively. The dopants Cu and Se ions do not show peaks because of less concentration but reference cards No. (00-051-1389) and (00-004-0836) show resemblance for Se and Cu respectively.

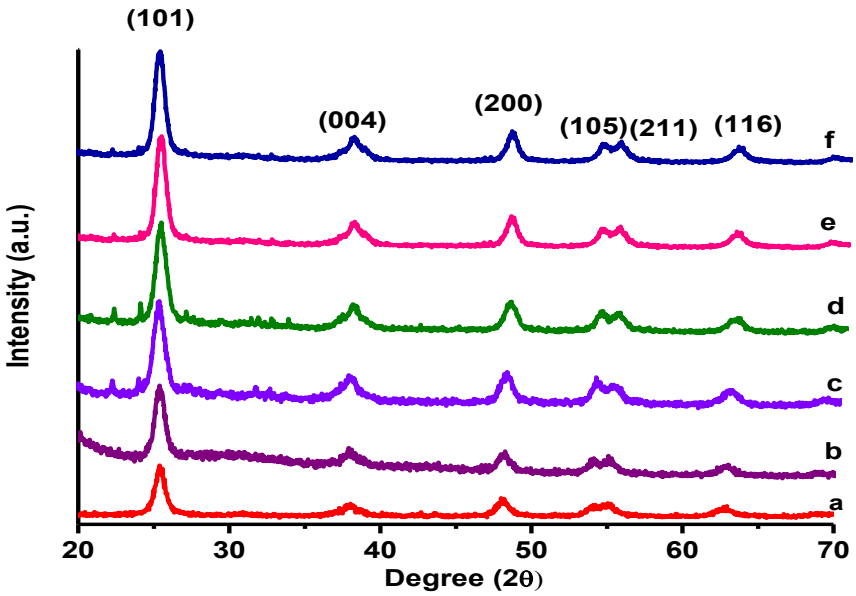

Figure 4.1 XRD of a) pure TiO_2, b) Cu-1% TiO_2, c) Cu-3% TiO_2, d) Cu-5% TiO_2, e) Cu-7% TiO_2, f) Cu-10% TiO_2.

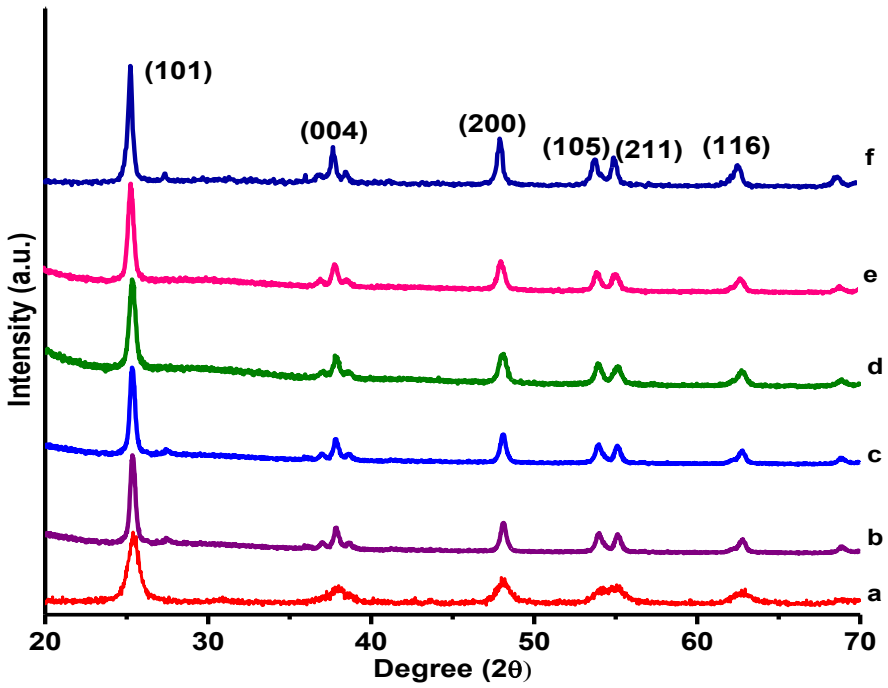

Figure 4.2 XRD of a) pure TiO_2, b) Se-1% TiO_2, c) Se-3% TiO_2, d) Se-5% TiO_2, e) Se-7% TiO_2, f) Se-10% TiO_2.

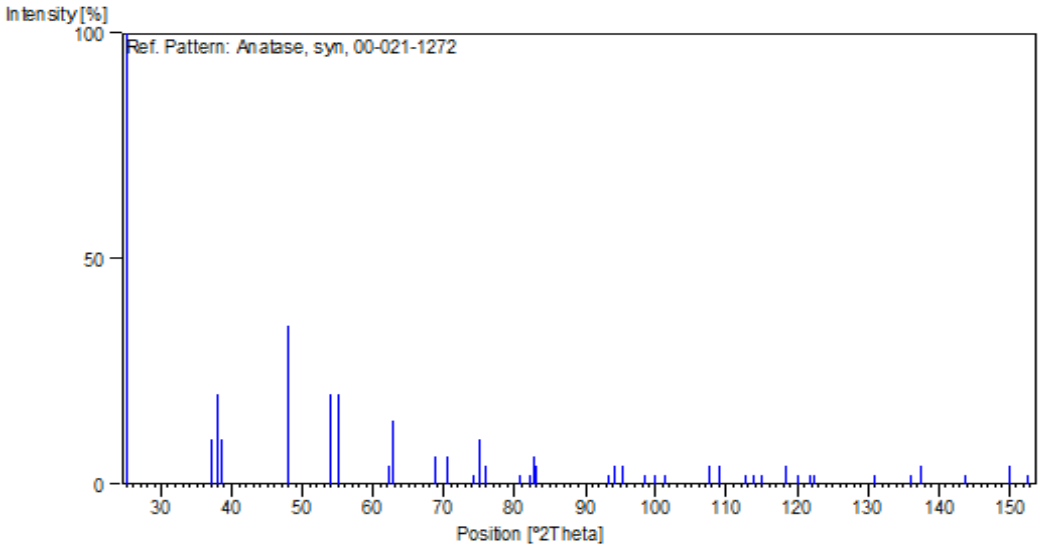

Figure 4.3 Stick pattern of anatase TiO_2.

Average crystallite size of all the catalysts were calculated by Scherrer's formula [86] which is

$$D = k\lambda/\beta \cos\theta$$

k = Scherrer constant. It's a shape factor and value is close to unity but varies with shape of crystallite.

λ = Wavelength of x-rays used (Cu k-alpha are mostly used having wavelength of 0.15405 nm)

β = Full width half maximum (FWHM) of observed peak

θ = Diffraction angle

Crystallite size range from 22-19 nm. Pure TiO_2 has crystallite size of 22 nm and doping lowers the size upto 19 nm. One thing that was observed was the slight shift in the diffraction angles of peaks of doped samples. This was because of incorporation of Cu and Se ions into the TiO_2 lattice that cause a change in cell volume and cell parameters of TiO_2 crystal lattice.

Table 4.1 Crystallite size of pure and doped nanocatalysts.

Sr. No.	**Sample code**	**Peak position[2θ]**	**FWHM**	**Average Crystallite size of peak**	**Average Crystallite size of Cu and Se doped TiO_2 (nm)**
1	TiO_2 NPs	25.41	0.78	10.81	22.33
		30.90	0.94	9.12	
		37.96	0.62	13.94	
		43.61	0.47	18.93	
		48.08	0.62	14.43	
		53.99	0.62	14.79	
2	Cu-1%	25.50	0.70	12.01	12.7
		37.83	0.62	13.93	
		48.17	0.62	14.44	
		55.25	0.62	14.88	
		53.99	0.62	14.79	
		62.68	1.15	8.43	
3	Cu-3%	25.40	0.86	9.83	12.1
		37.95	0.62	13.94	
		48.16	0.78	11.55	
		53.93	0.62	14.79	
		55.29	0.78	11.90	

		62.66	0.94	10.29	
4	Cu-5%	25.29	0.86	9.82	11.22
		37.85	0.55	15.93	
		48.02	0.62	14.43	
		53.92	0.62	14.79	
		55.13	0.62	14.87	
		68.84	0.94	10.65	
5	Cu-7%	25.47	0.86	9.83	13.6
		37.79	0.55	15.92	
		48.24	0.62	14.44	
		53.94	0.62	14.79	
		55.19	0.78	11.90	
		68.84	0.62	15.98	
6	Cu-10%	25.47	0.51	16.63	14.2
		37.79	0.55	15.92	
		48.24	0.62	14.44	
		53.94	0.62	14.79	
		55.19	0.78	11.90	
		68.84	0.78	12.78	
7	Se-1%	25.31	0.35	24.02	20.666
		37.84	0.31	27.87	
		48.11	0.31	28.87	
		53.93	0.39	23.67	
		55.10	0.39	23.79	
		62.79	0.39	24.71	
8	Se-3%	25.32	0.47	18.01	19.954
		37.84	0.31	27.87	
		48.03	0.55	16.49	
		53.93	0.47	19.72	
		55.13	0.55	17.00	
		62.80	0.47	20.59	
9	Se-5%	25.32	0.47	18.01	19.386
		37.84	0.31	27.87	
		48.03	0.55	16.49	
		53.93	0.47	19.72	

		55.13	0.55	17.00	
		62.80	0.47	20.59	
10	Se-7%	25.32	0.47	18.01	19.344
		37.84	0.31	27.87	
		48.03	0.47	16.49	
		53.93	0.39	19.72	
		55.13	0.47	17.00	
		62.80	0.55	20.59	
11	Se-10%	25.29	0.39	21.62	21.21
		37.86	0.39	22.30	
		48.08	0.47	19.25	
		53.98	0.39	23.67	
		55.08	0.47	19.82	
		62.81	0.47	20.59	

The composition and purity of all these doped nanocatalysts are also confirmed by energy dispersive x-ray spectroscopy analysis. EDX of Cu and Se doped TiO_2 is shown in **fig 4.4** and **4.5**. All the peaks correlate with Titanium, Oxygen, Cu and Se. Only in some samples instrumental peaks of carbon was observed. The **table 4.2** shows the EDX of Cu-7% having elements of Ti, Cu and a small amount (1.58 %) of sulphur because precursor for the Copper doping used was $CuSO_4.5H_2O$ all of these combine to form 100%. Similarly **table 4.3**.shows the EDX for Se doped TiO_2 showing peaks of Ti, O and Se forming total 100% atomic ratio.

Table 4.2 EDX of Cu-7% doped TiO_2

Elements	Weight%	Atomic%
S K	1.05	1.58
Ti K	96.42	96.52
Cu K	2.52	1.90
Totals	100.00	

Table 4.3 EDX of Se-7% doped TiO_2

Elements	Weight%	Atomic%
O K	56.67	79.77
Ti K	42.54	20.00
Se L	0.79	0.23
Totals	100.00	

The EDX shown in **table 4.2** of Cu-7% have an atomic percentage of Ti 96.52 %, Cu is 1.90% and sulphur atomic percent is 1.58%. The signal of sulphur is may be because of precursor used for Cu doping was $CuSO_4.5H_2O$. In case of Se-7% doping shown in **table 4.3** it was observed that atomic percentage if Se, Ti and O are 0.23, 20.00 and 79.77 respectively.

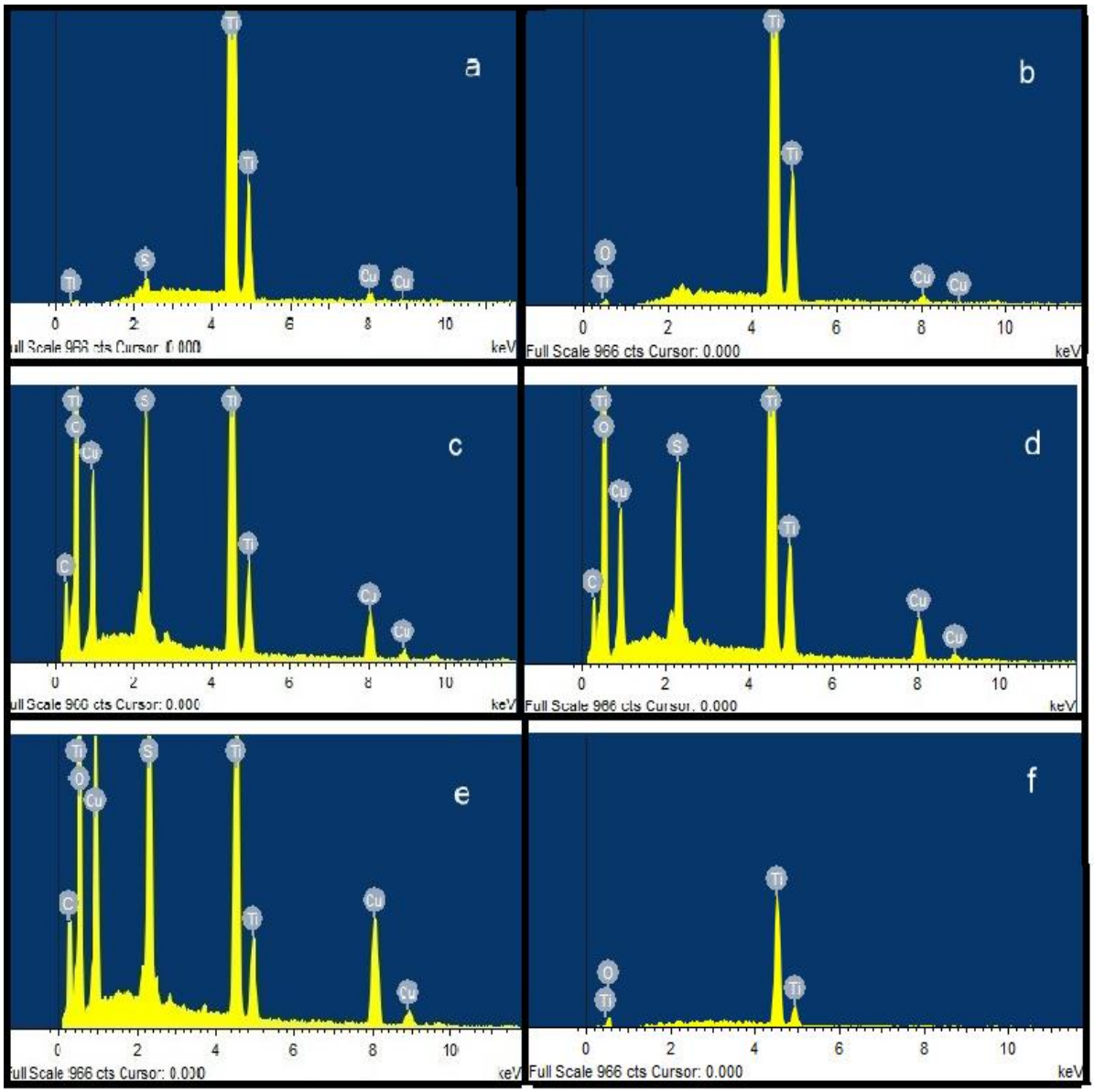

Figure 4.4 EDX analysis of a) Cu-1% TiO_2, b) Cu-3% TiO_2, c) Cu-5% TiO_2, d) Cu-7% TiO_2, e) Cu-10% TiO_2 f) pure TiO_2

EDX if pure TiO_2 in **fig 4.4(f)** shows that only the peak of Ti and Oxygen are present in sample while in all tha other spectras from a to e as the dopant concentration i.e of Cu is increasing the peak of Cu appared at number 9 on x-axis also increased gradually.

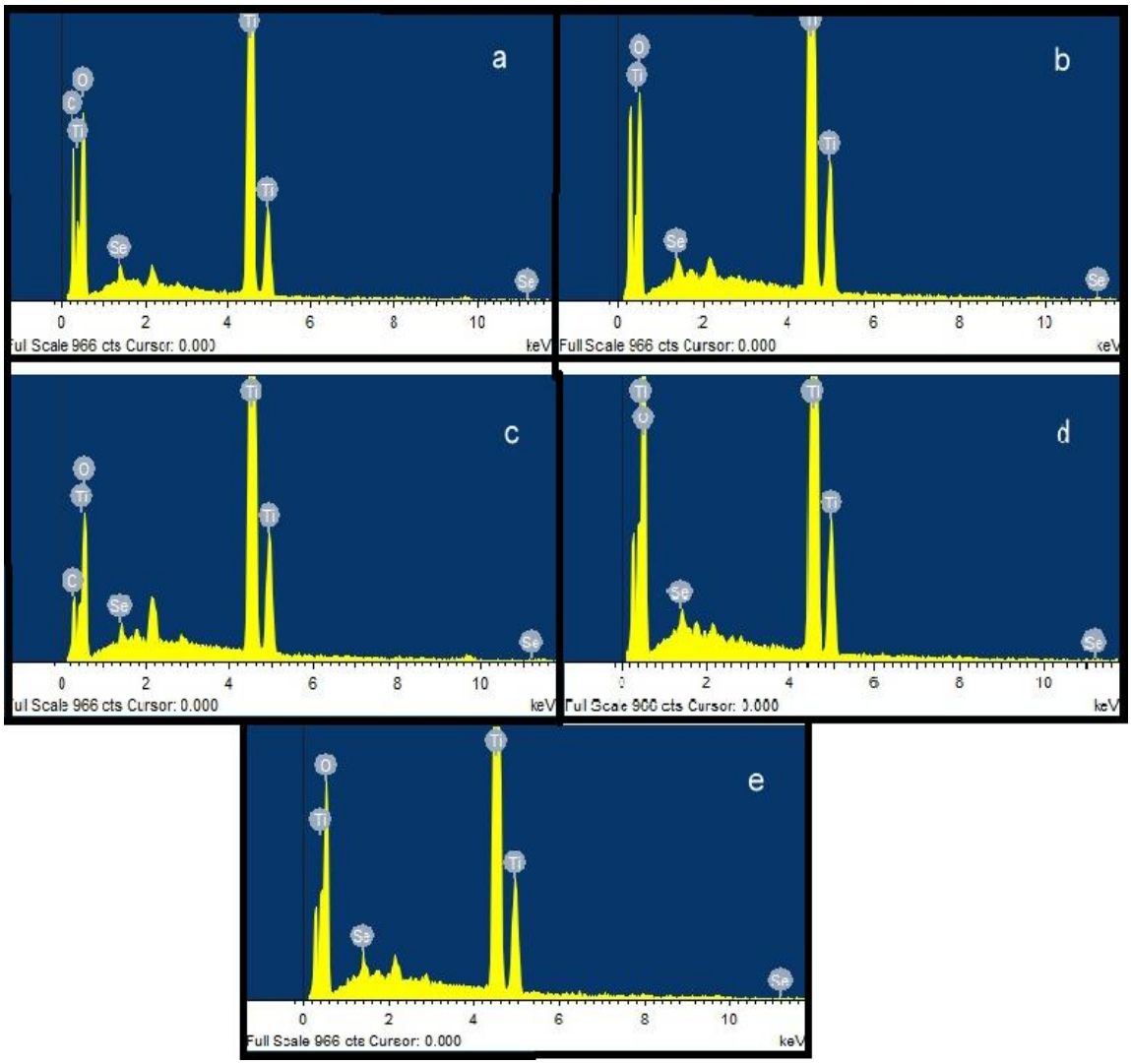

Figure 4.5 EDX analysis of a) Se-1% TiO_2, b) Se-3% TiO_2, c) Se-5% TiO_2, d) Se-7% TiO_2, e) Se-10% TiO_2.

EDX of Se doped TiO_2 is shown in **fig 4.5** as the dopant concentration is increasing from **fig 4.5 a to e** the peak of Se observed at 1.7 in x-axis also increased in intensity. Tha peak that appear at start of spectra near to 0 value in x-axis shows that the elctrons during EDX are removed from the K-shell.

4.2 Morphological analysis

SEM images of pure and doped TiO_2. The average particle size of TiO_2 was 61.1 nm and that of doped TiO_2 is ranging from 45-37 nm. It was observed that doping decreases the particle size significantly. The morphology of pure TiO_2 was spherical but the doped particle become more like aggregated plates. Agglomeration was also seen in samples that was probably because of nucleation during hydrolysis or heat treatment. In Cu-doped sample **fig 4.6 and 4.7** the surface was rough and roughness increases as Cu content was increased. But greater surface roughness is good for photocatalytic activity as it bound to the reactants more efficiently [87]. Cu doping also effect the catalyst by decreasing grain size and inturn increasing surface area which again leads to more photo catalytic activity. Se doped samples **fig 4.8** and **4.9** show spherical particles but agglomerated.

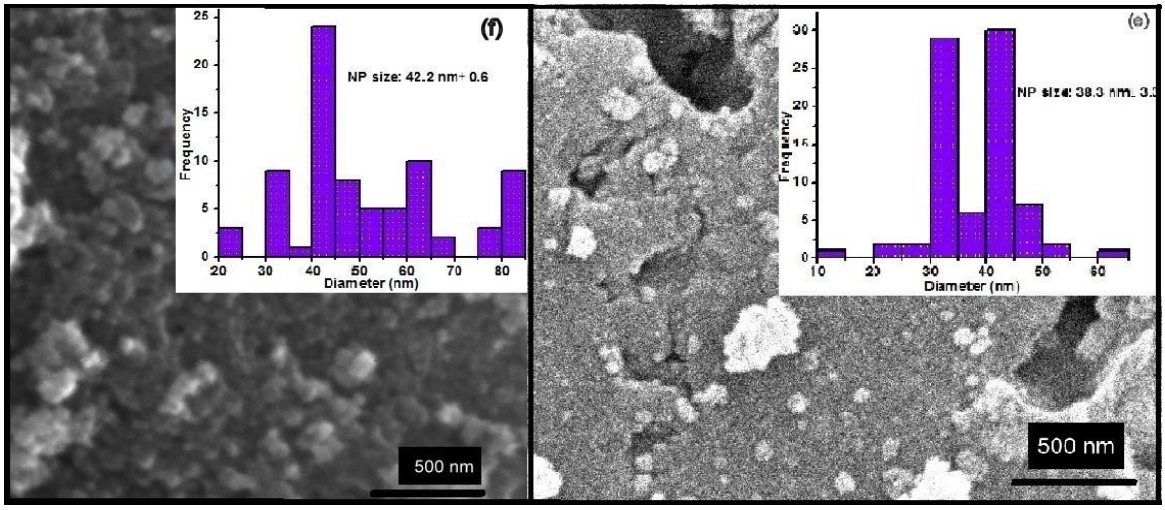

Figure 4.6 e) Cu-7% TiO_2, f) Cu-10% TiO_2.

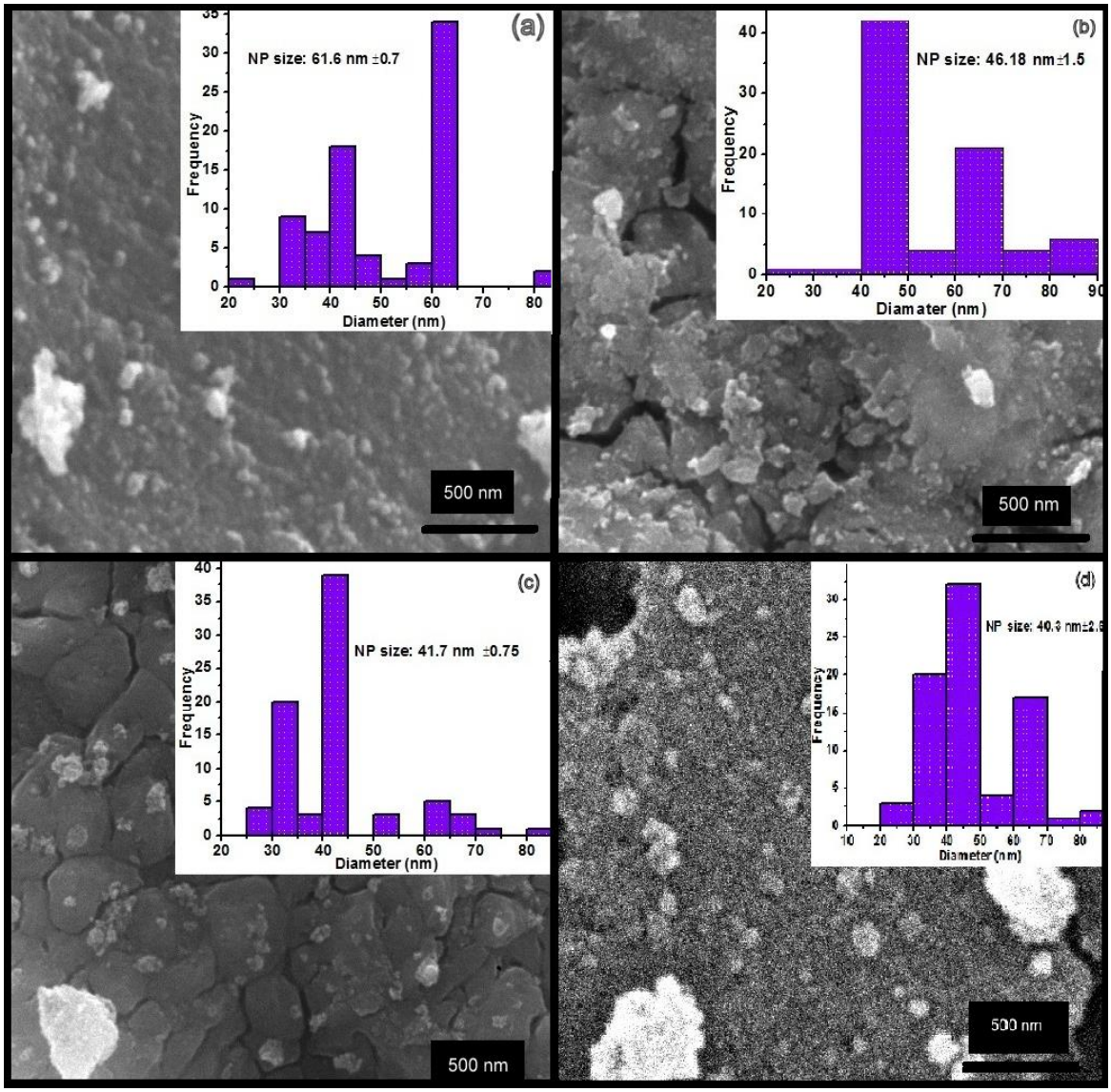

Figure 4.7 SEM analysis of a) pure TiO_2, b) Cu-1% TiO_2, c) Cu-3% TiO_2, d) Cu-5% TiO_2.

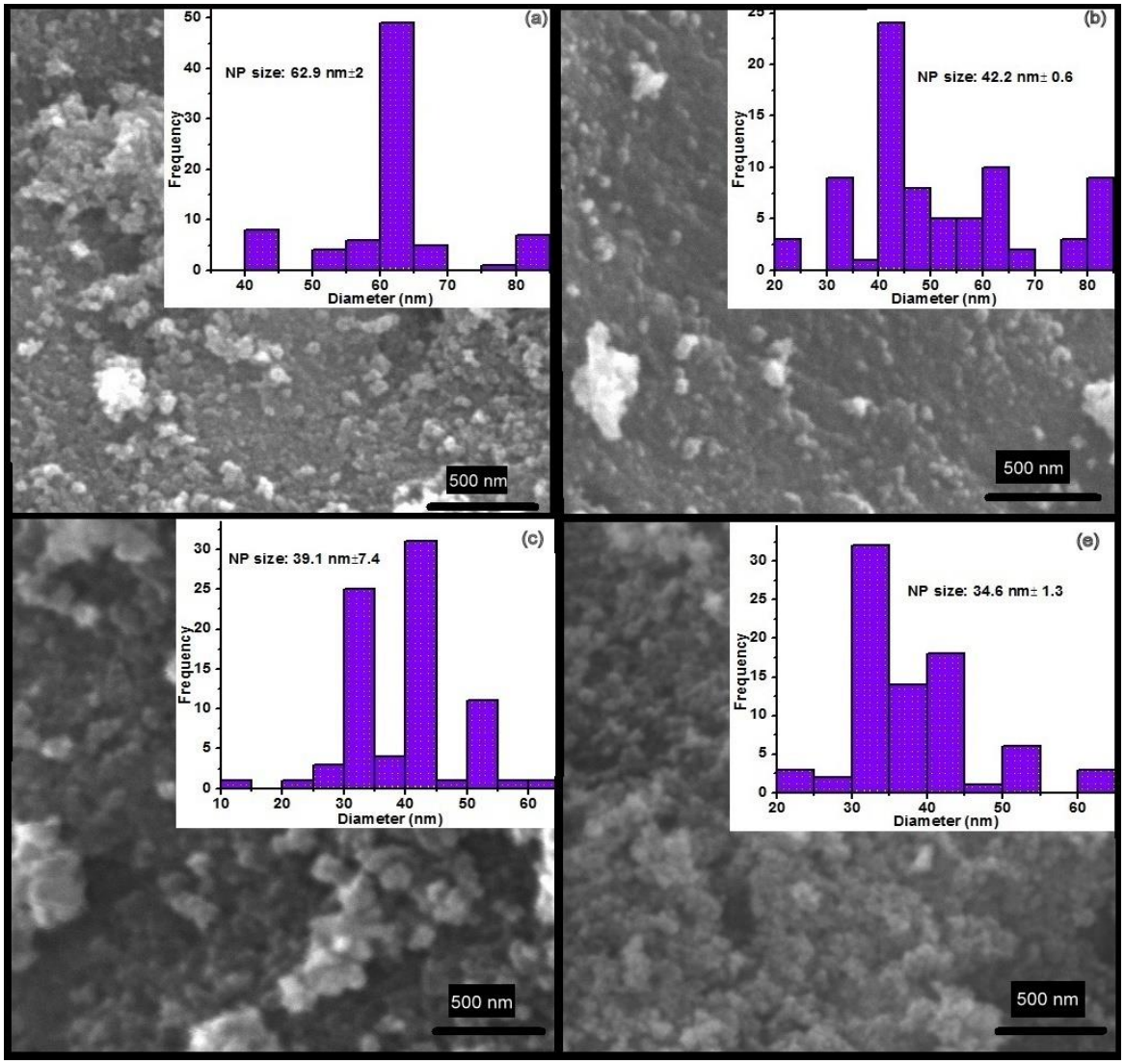

Figure 4.8 a) Se-1% TiO_2, b) Se-3% TiO_2, c) Se-5% TiO_2 e)Se-10% TiO_2.

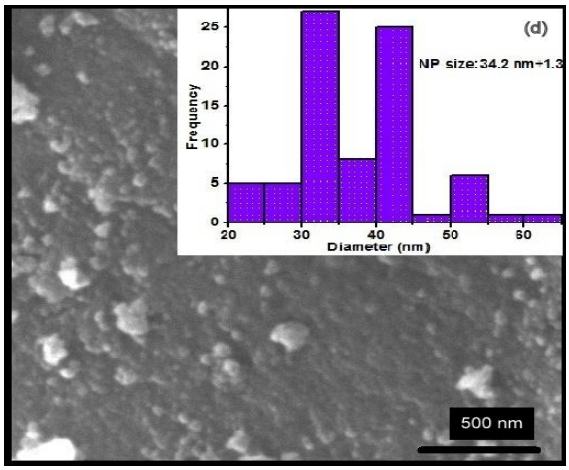

Figure 4.9 d) Se-7% TiO_2

4.3 Optical properties

The absorbance of pure and doped TiO_2 was determined by adding 0.5 mg of catalyst in 10 ml of methanol. The catalysts were sonicated for about 30 mins to get better suspension. A milky suspension was formed after sonication. The absorption was checked between 200-700 nm using UV-Vis spectroscopy. TiO_2 nanoparticles show a strong absorption edge at 387 nm. Band gap of TiO_2 is 3.20 eV and absorb UV- light which is less than 5% in electromagnetic spectrum. To make catalyst more efficient and productive. Tuning its band gap was necessary. An impurity atom was added in the form of dopant to lower its band gap so that it can absorb visible light. The doped samples show absorbance more towards red shift. Forming a strong absorption edge between 400-450 nm as the dopant content was increased. Absorbance and tauc plots of all the Cu doped catalysts were shown in **fig 4.10**, **4.11** and **4.12**

Tauc plots were formed from absorbance using the equation

$$E=hc/\lambda$$

$$\text{As } 1 \text{ eV} = 1.60 \times 10^{-19} \text{ J}$$

$$hc = (6.62 \times 10^{-34} \text{ Js}).\ (3\times10^{8} \text{ m/s})$$

$$= 6.62 \times 10^{-34}.\ (1.6 \times 10^{-19})\ (3 \times 10^{8} \text{ m/s})$$

$$= 1.24 \text{ eV} \times 10 -6 = 1240 \text{ V.nm}$$

$$=1240/\lambda = \text{band gap in eV}$$

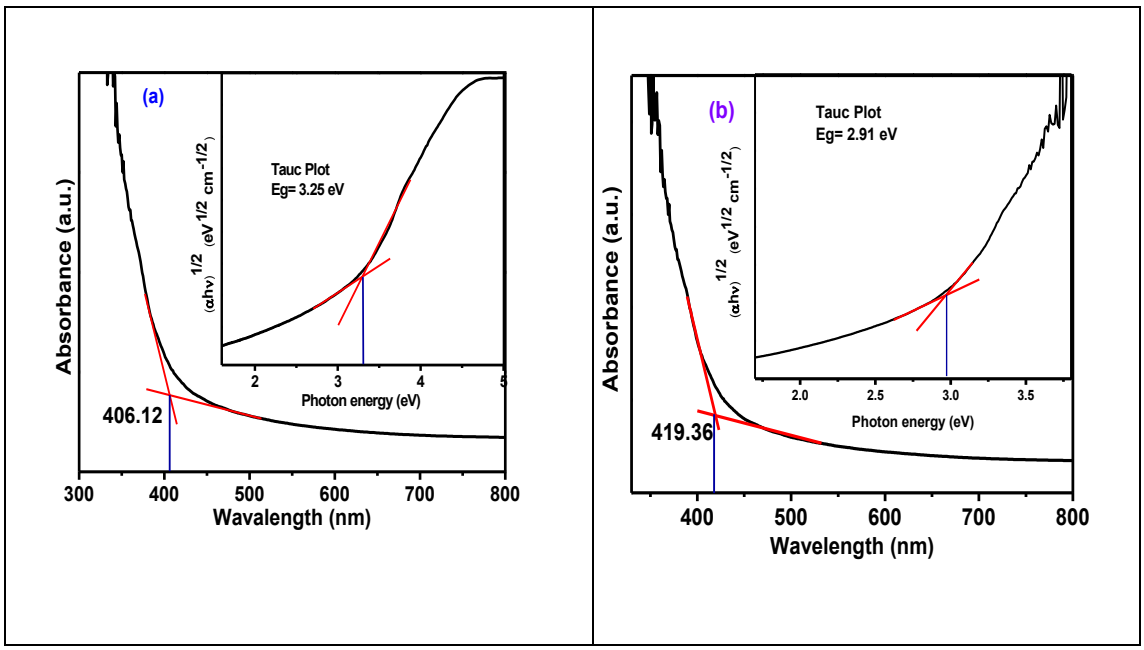

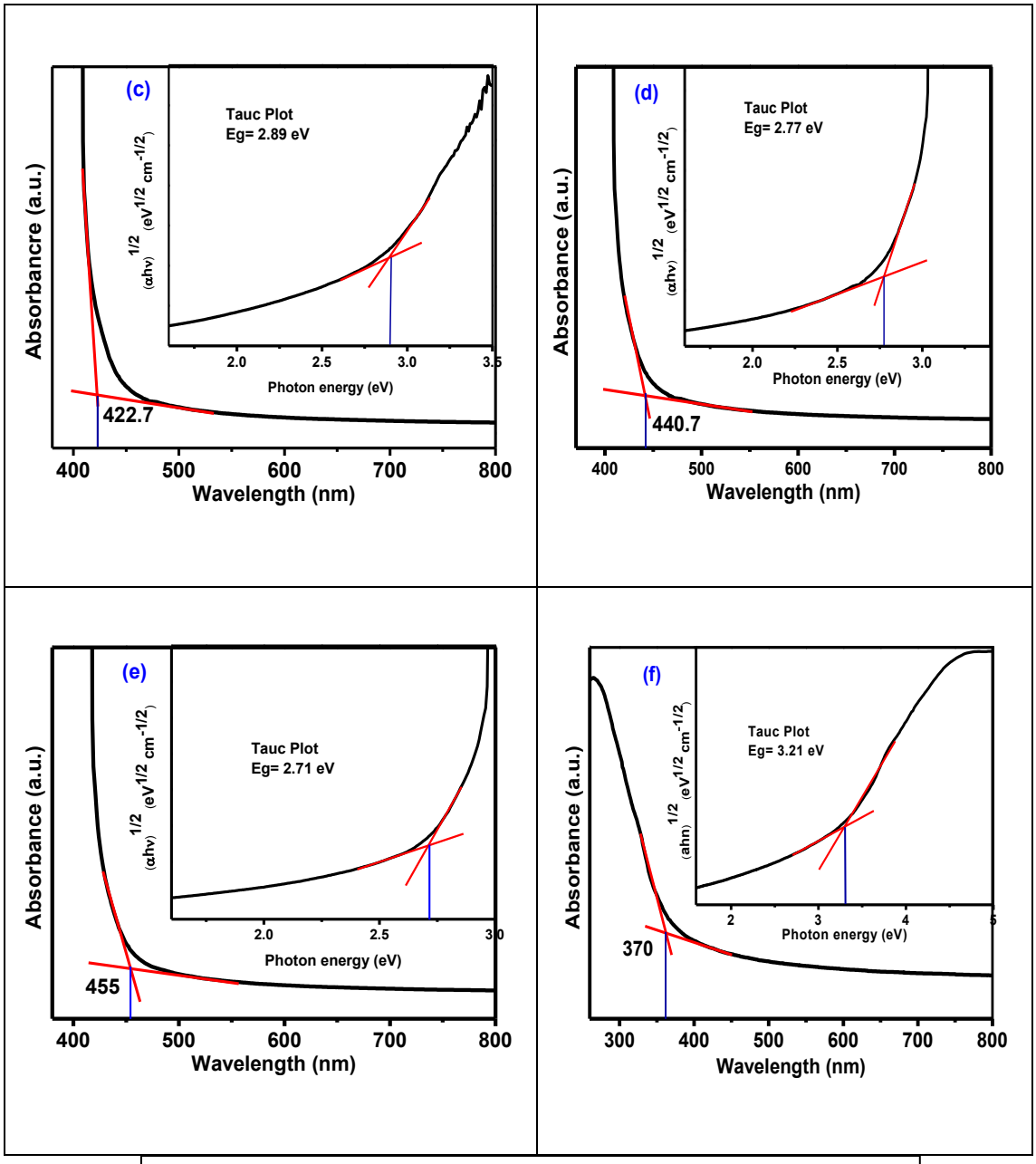

Figure 4.10 Absorbance and Tauc plots of a) Cu-1%, b) Cu-3%, c) Cu-5%, d) Cu-7%, e) Cu-10%, f) TiO_2 Nps

Dopants introduce internal band gaps that decrease recombination rate and this introduction was evident from red-shift Cu and Se ions exist in the forms of Cu^{2+} and Cu^{+} and Se^{2+} individually so they behave as electron trappers. This incorporation of dopants increase the photocatalytic activity but at high Cu levels they become recombination centers making electron and hole recombination rate faster.

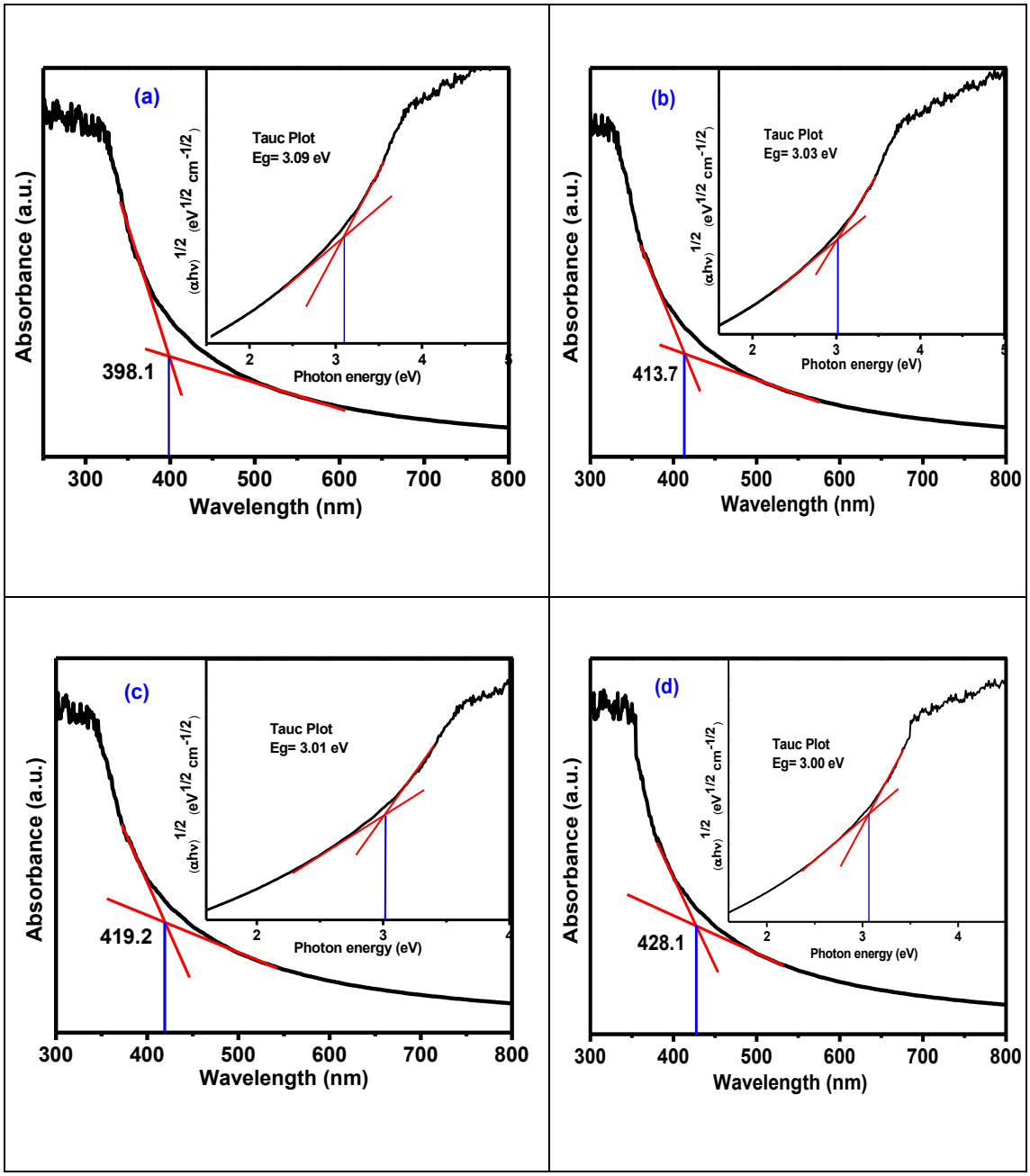

Figure 4.11 Absorbance and Tauc plots of a) Se-1%, b) Se-3%, c) Se-5%, d) Se-7% TiO_2

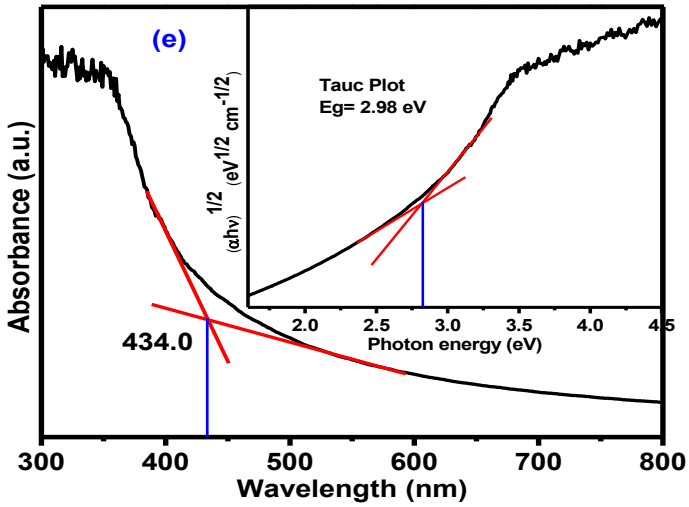

Figure 4.12 Absorbance and Tauc plot of e) Se-10% TiO_2

.

4.3 Surface area analysis

N_2 gas adsorption desorption gives us information about surface area of paricles. For BET model Gemini VII 2390 NOVA 2200e Quanta Chrome was used. Before analysis the samples were degassed at 200 ^{o}C for overnight to remove moisture and all organic impurities. After that a measured quantity of sample not less than 0.2 mg was taken in a tube. Nitrogen gas was passed from samples at relative pressure (p/p°) range of 0.02 to 0.9 which is best to determine surface area. It was observed from **table 4.4** that the surface area gradually increases by increasing the dopant ratio and then decreased at ratio of Cu-10% and Se-10%. The plot against Relative Pressure (p/p°) and 1/[Q(p°/p - 1)] is shown in **fig 4.13** and **4.14.**

Table 4.4 BET surface area of Cu-doped samples

Sample code	**BET surface area (m^2/gm)**	**Pore size (Å)**
Cu-1%	37.52	14.83
Cu-3%	39.89	14.83
Cu-5%	44.03	14.83
Cu-7%	59.32	14.83
Cu-10%	43.71	14.83

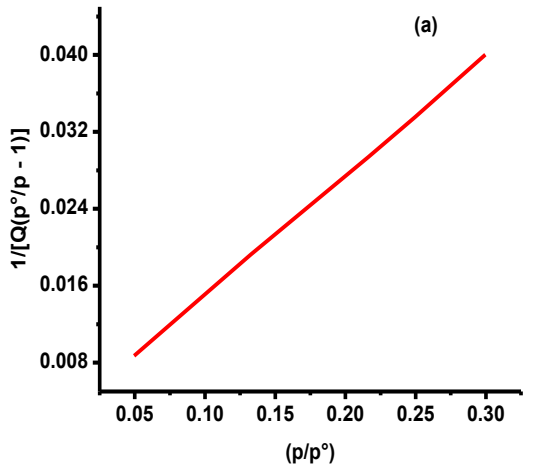

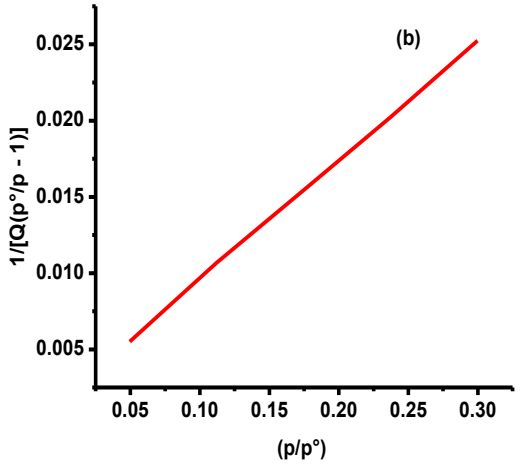

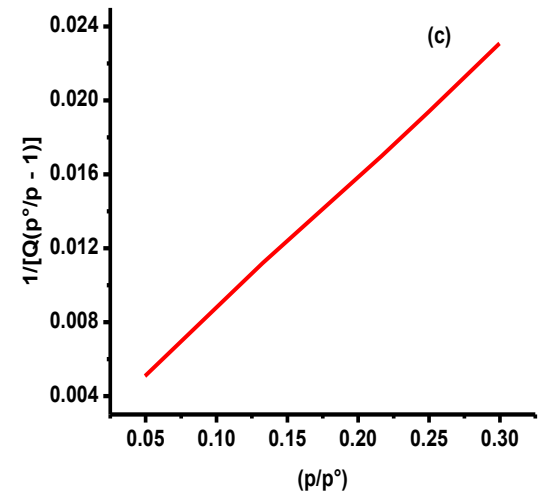

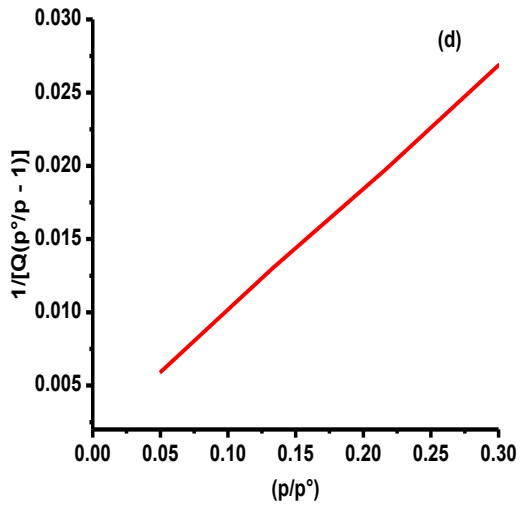

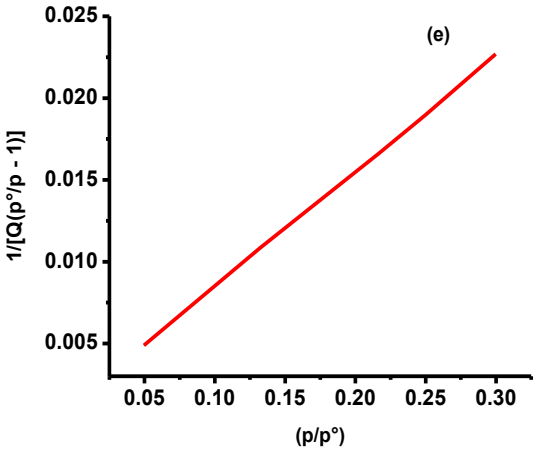

Figure 4.13 BET graphs of (a) Cu-1%, (b) Cu-3%, (c) Cu-5%, (d) Cu-7%, (e) Cu-10% doped TiO_2.

Table 4.5 BET surface area of Se doped samples

Sample code	BET surface area (m^2/g)	Pore size (Å)
Se-1%	34.25	19.30
Se-3%	54.35	19.30
Se-5%	59.56	19.25
Se-7%	80.38	144.86
Se-10%	60.38	19.32

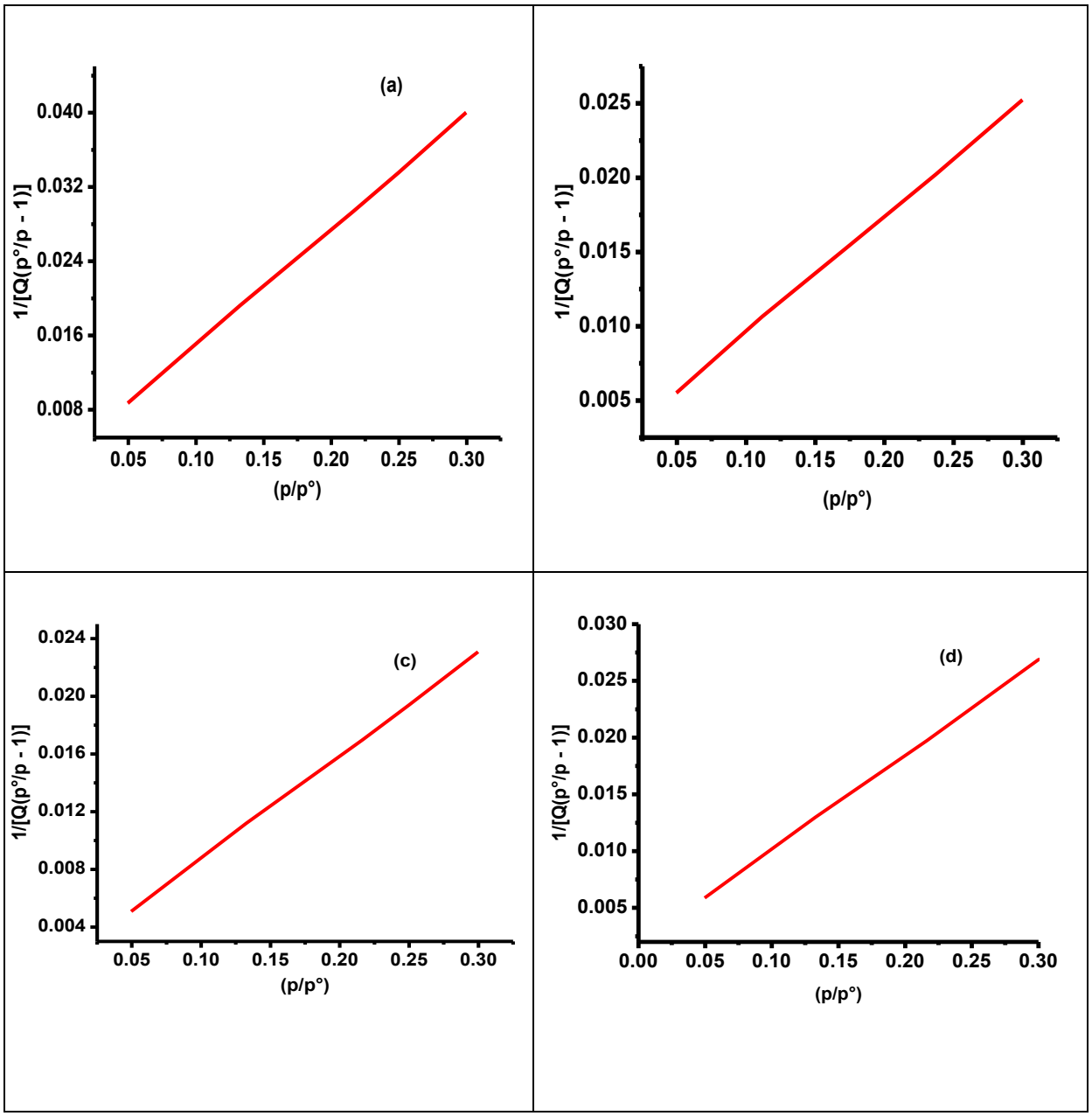

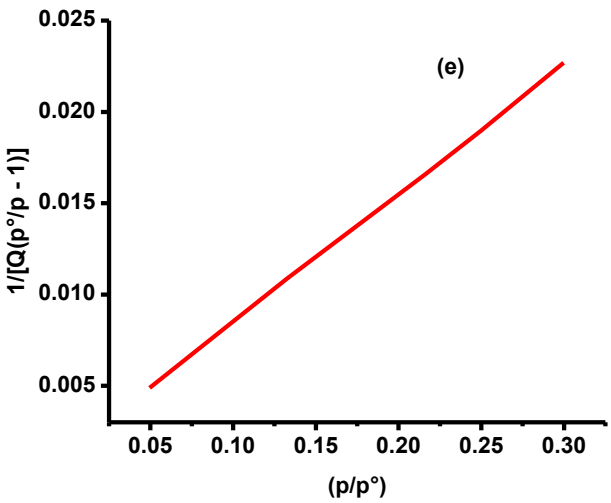

Figure 4.14 BET graphs of (a) Se-1%, (b) Se-3%, (c) Se-5%, (d) Se-7% and (e) Se-10% doped TiO_2.

Degradation studies

To apply the optical perties of nano-catalyst degradation studies were carried out on methyl orange and glyphosate. For both dye and pesticide 0.1 mM solution was made from stock solution which was further diluted up to 0.01mM. So for all catalysts 50 mg of catalyst was taken in 50 ml of water and dye solution. But its quite clear from literature that for better degradation the dye or pesticide molecules need to be adsorbed on the surface of catalyst for efficient charge transfer [88]. For this the catalyst and pollutant mixture was stirred in the dark for about 60 mins to achieve absorption- desorption equilibrium. After that the samples were place on orbital shaker for continuous stirring and in photo reactor having 3-LED (each of 150 W) as shown in **fig 4.15(a).** 5ml solution was taken after regular intervals, centrifuged for 10 mins at 10000 rpm and absorbance was measured.

It was observed from the degradation studies that all dopant samples show more degradation than undoped TiO_2 and if doped samples were compared with each other TiO_2 with 7% dopant ratio show best photocatalytic activity. If the dopant ratio was increased further i.e. upto 10%. The degradation doesn't increase. The reason of low photocatalytic activity can be the production of CuO and CuO_2. More dopant concentration also leads to side products like CuO and CuO_2 which than deposite on the surface of catalyst and cause less sunlight to reach on the surface of nano catalyst. Also degradation depends on mber of

hydroxyl radicals and excess Cu^{2+} ions react with hydroxyl radicals forming $(Cu(H_2O)^{n+1}$. According to the literature they deposit on the surface decreasing the amount of OH radicals available [89]. Another reason for the low degradation can be that after reaching the optimal condition when the doping content is increased, the space charge region becomes notably narrow, and the penetration depth of light into TiO_2 greatly exceeds the space charge layer. Therefore, the recombination of the photo-generated electron–hole pairs becomes easier, and fewer charge carriers reach the surface to initiate the degradation phenomenon, which decrease the photocatalytic activity.

Figure 4.15(a) degradation of methyl orange under visible light

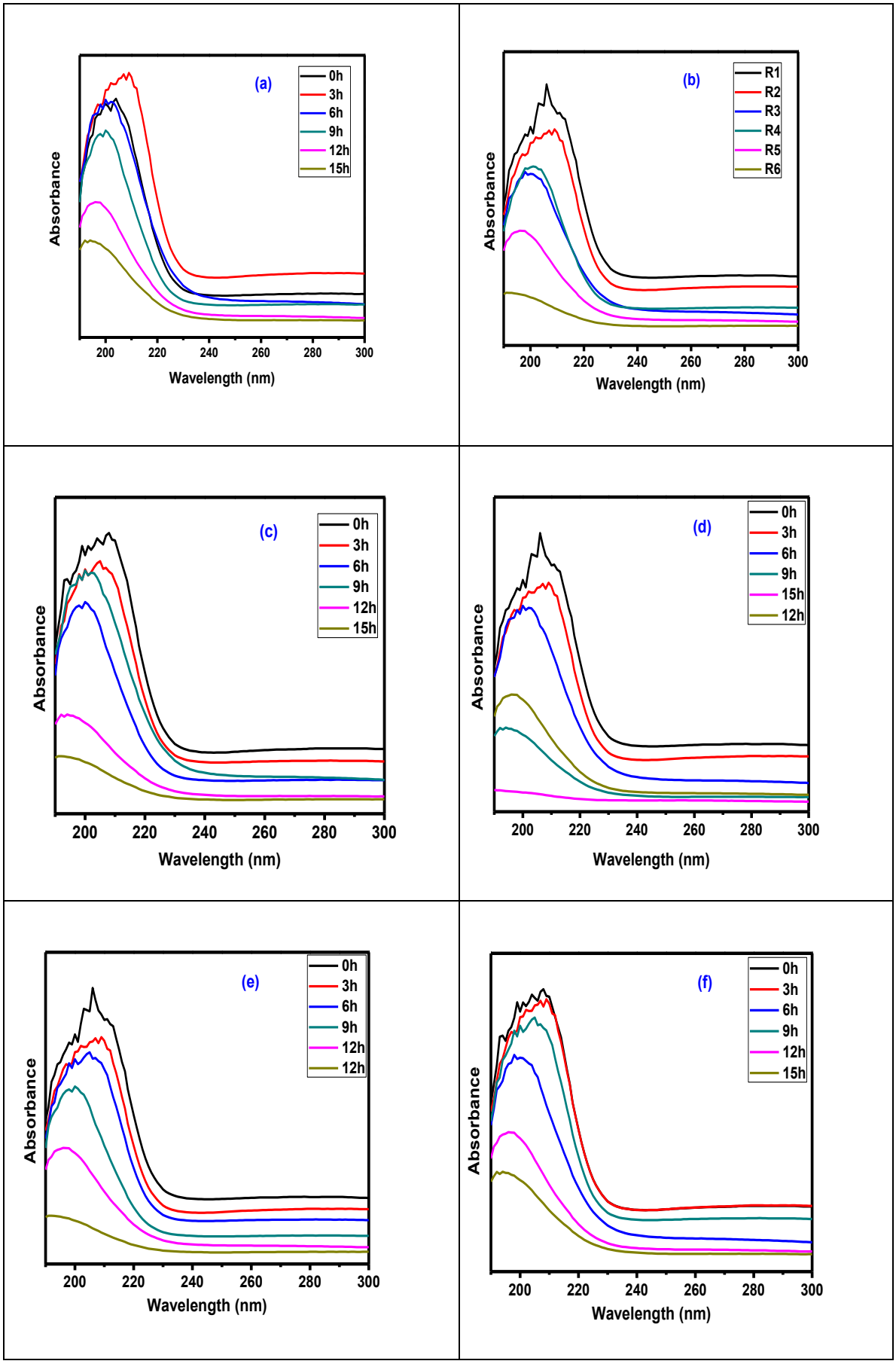

Figure 4.15(b) Degradation spectras of glyphosate using (a) Cu-1%, (b) Cu-3%, (c) Cu-5%, (d) Cu-7%, (e) Cu-10%, f) pure TiO_2.

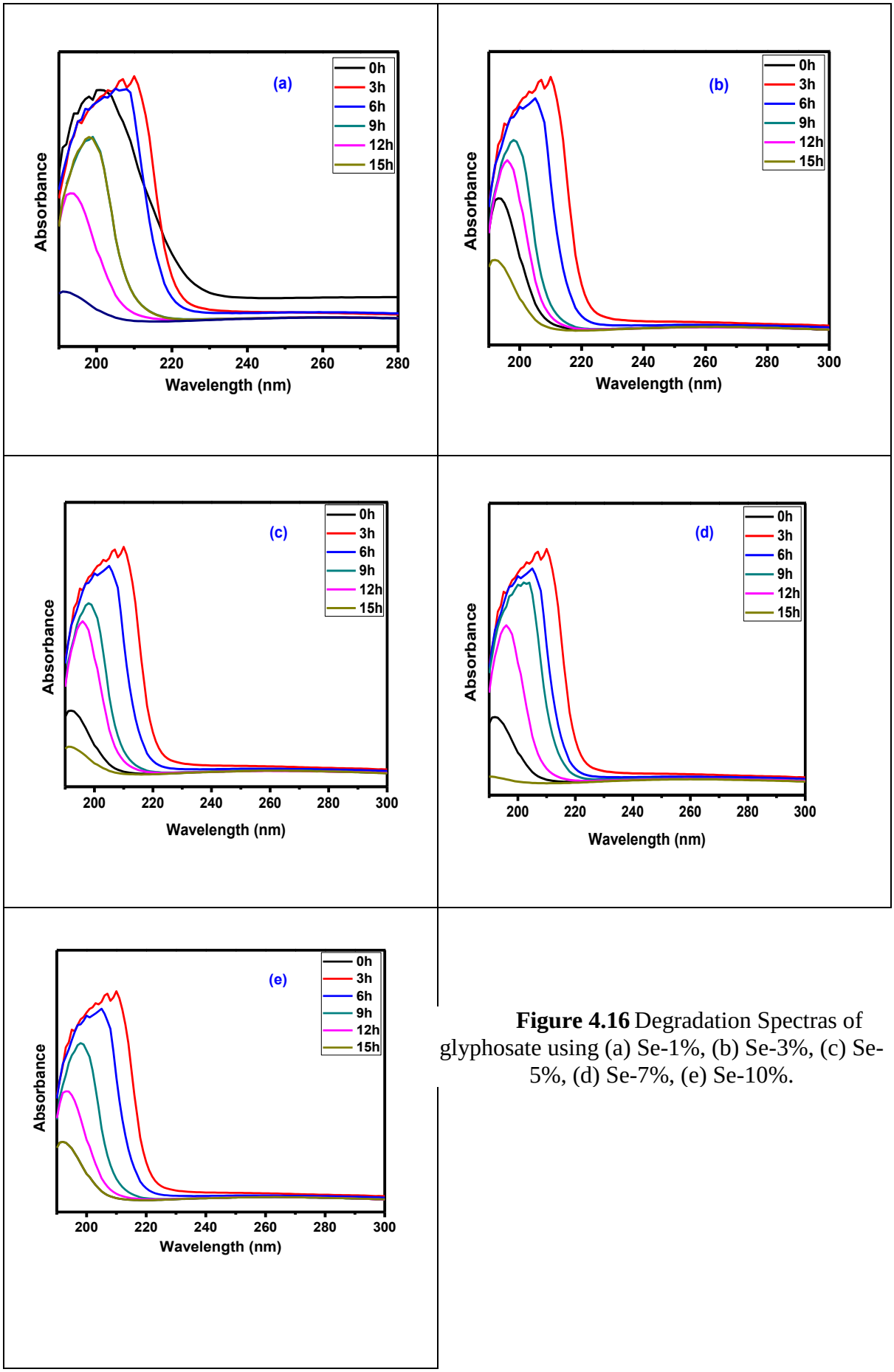

Figure 4.16 Degradation Spectras of glyphosate using (a) Se-1%, (b) Se-3%, (c) Se-5%, (d) Se-7%, (e) Se-10%.

Similarly the degradation studies were carried out on methyl orange using both Cu and Se catalysts. The maximum and characteristics absorbance of methyl orange is at 465, 464 nm. **fig 4.17** shows degradation studies of methyl orange using Cu doped TiO_2 series

fig 4.18 shows degradation of MO with Se doped TiO_2 series. The decrease in absorbance after every reading was observed which is very evident from graphs plotted of quantity absorbed verses wavelength.

Fig 4.15(b) and **4.16** shows the degradation of glyphosate using Cu doped and Se doped TiO_2 respectively. All degradation spectras show that nanocatalysts are working fine for glyphosate but Cu-7% and Se-7% are best of all nanocatalysts.

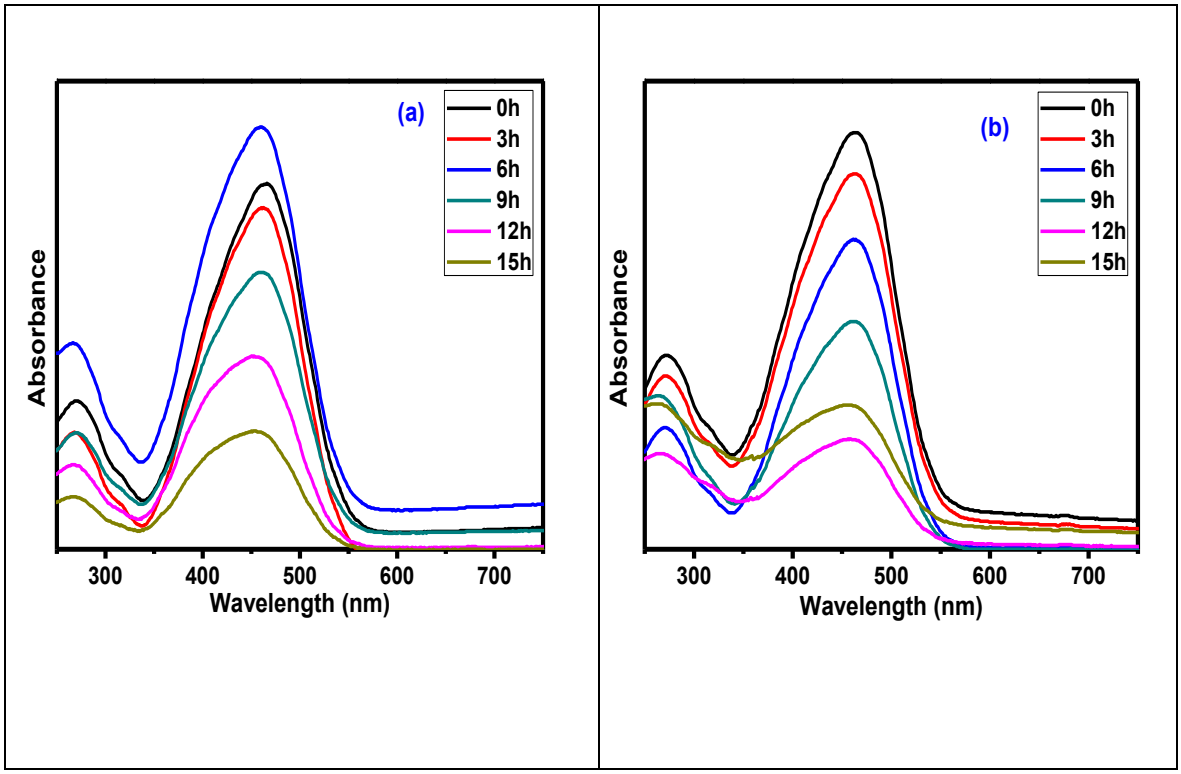

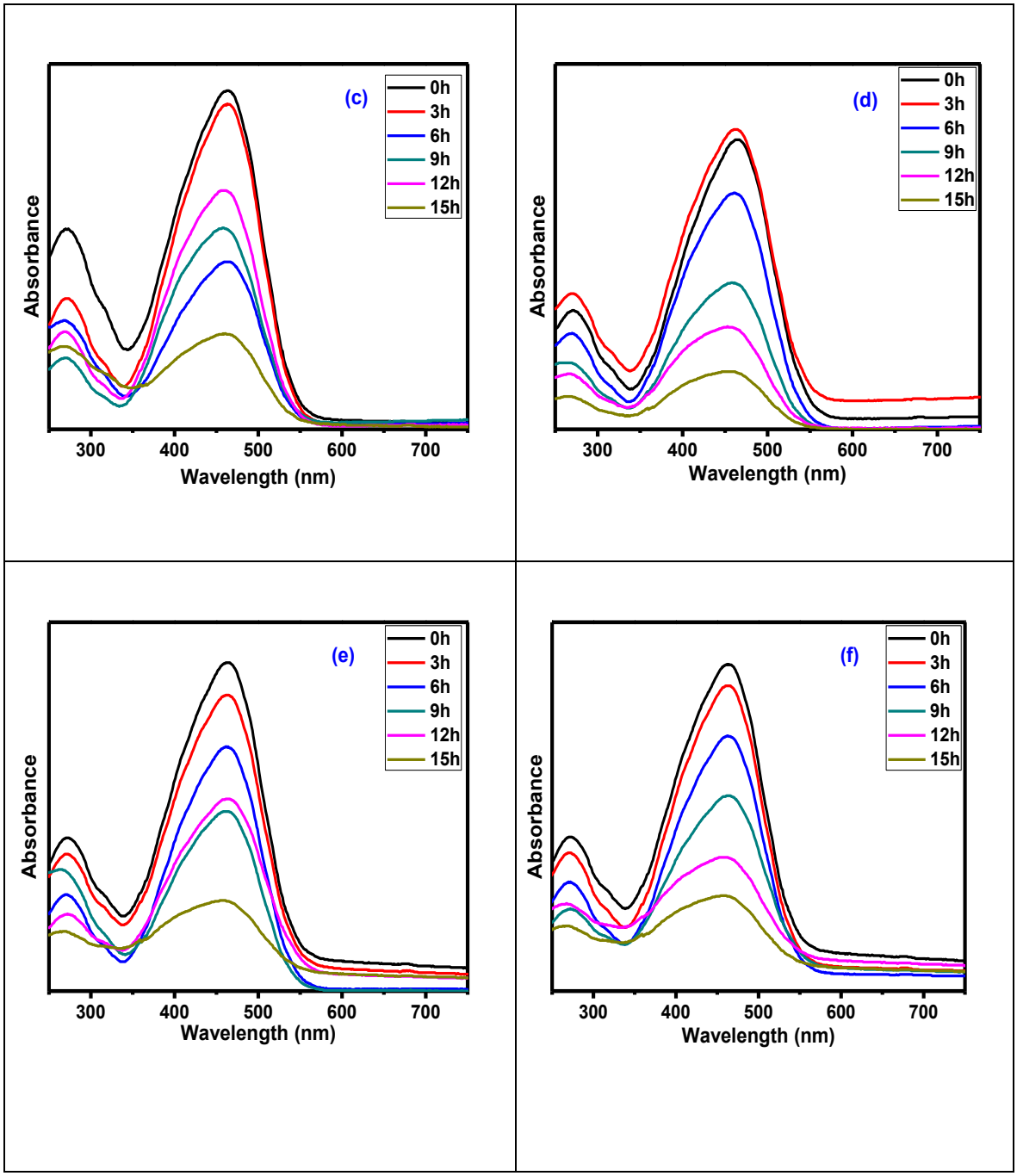

Figure 4.17 Degradation spectras of methyl orange using (a) Cu-1%, (b) Cu-3%, (c) Cu-5%, (d) Cu-7%, (e) Cu-10% and (f) pure TiO_2.

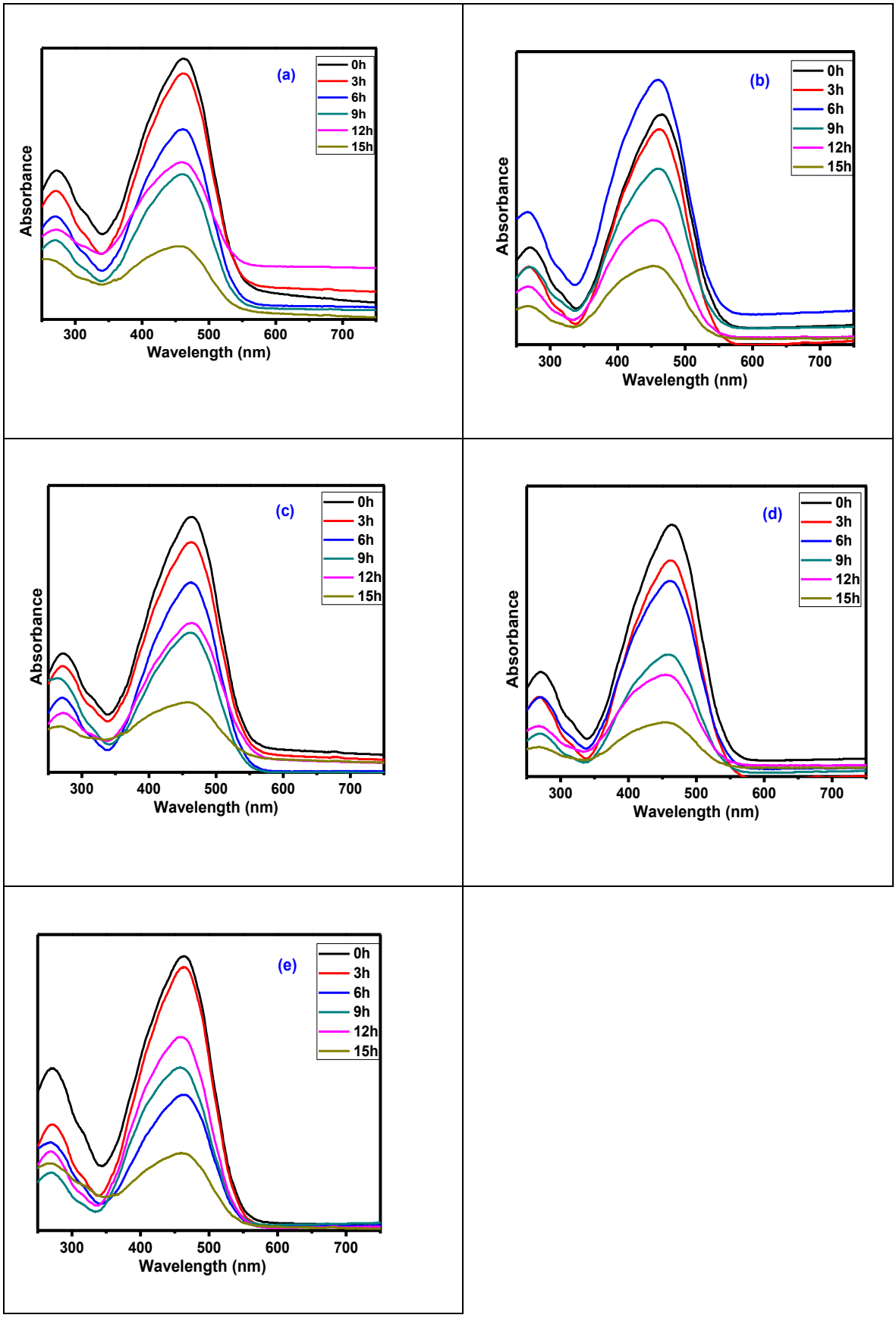

Figure 4.18 Degradation spectras of methyl orange using (a) Se-1%, (b)8Se-3%, (c) Se-5%, (d) Se-7%, (e) Se-10%.

.

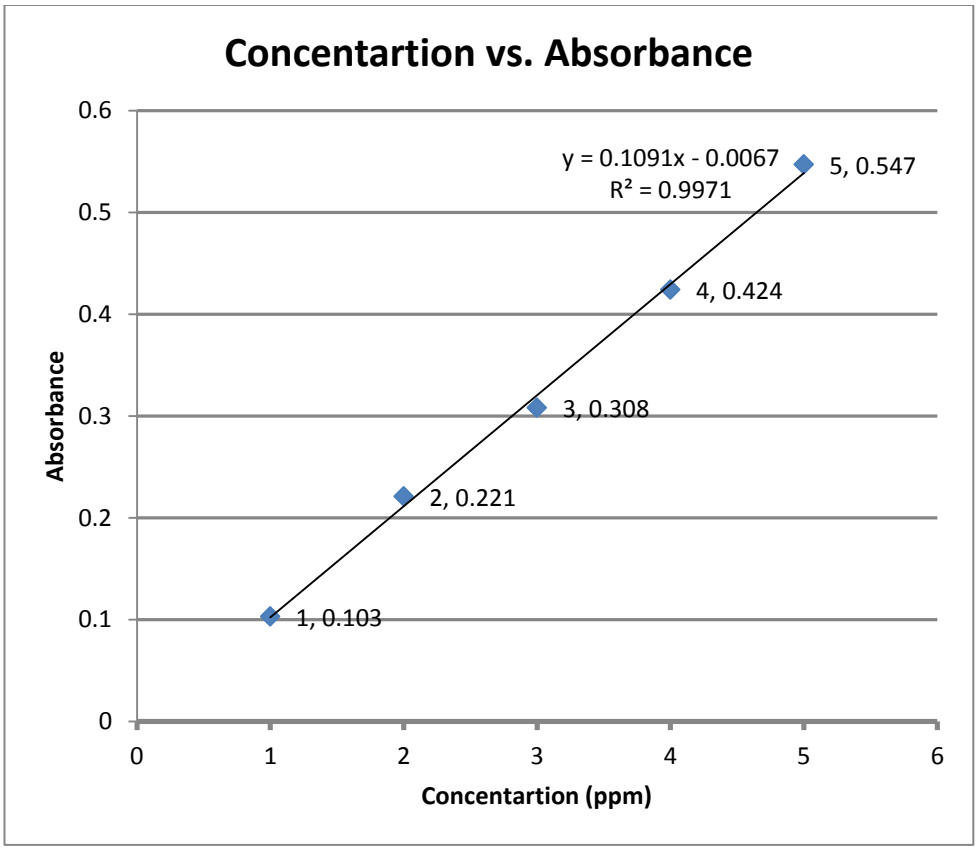

Figure 4.19 Calibration curve for glyphosate.

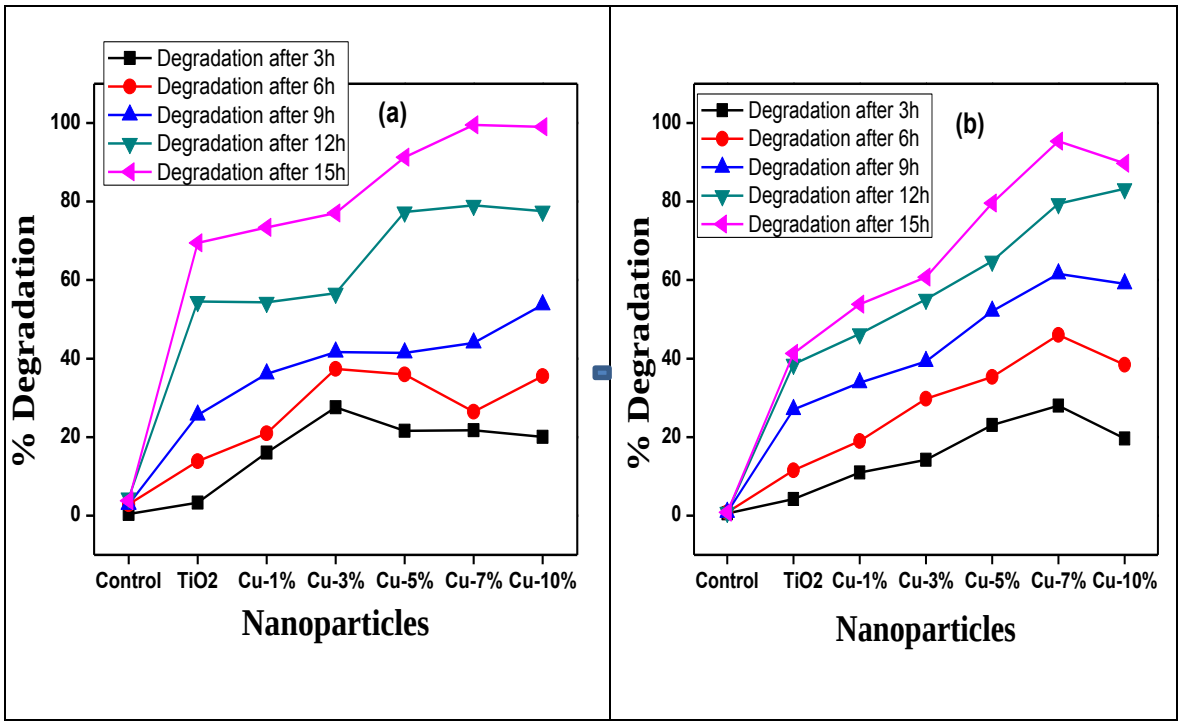

Figure 4.20 Efficiency of a) Cu and b) Se doped samples for Glyphosate degradation.

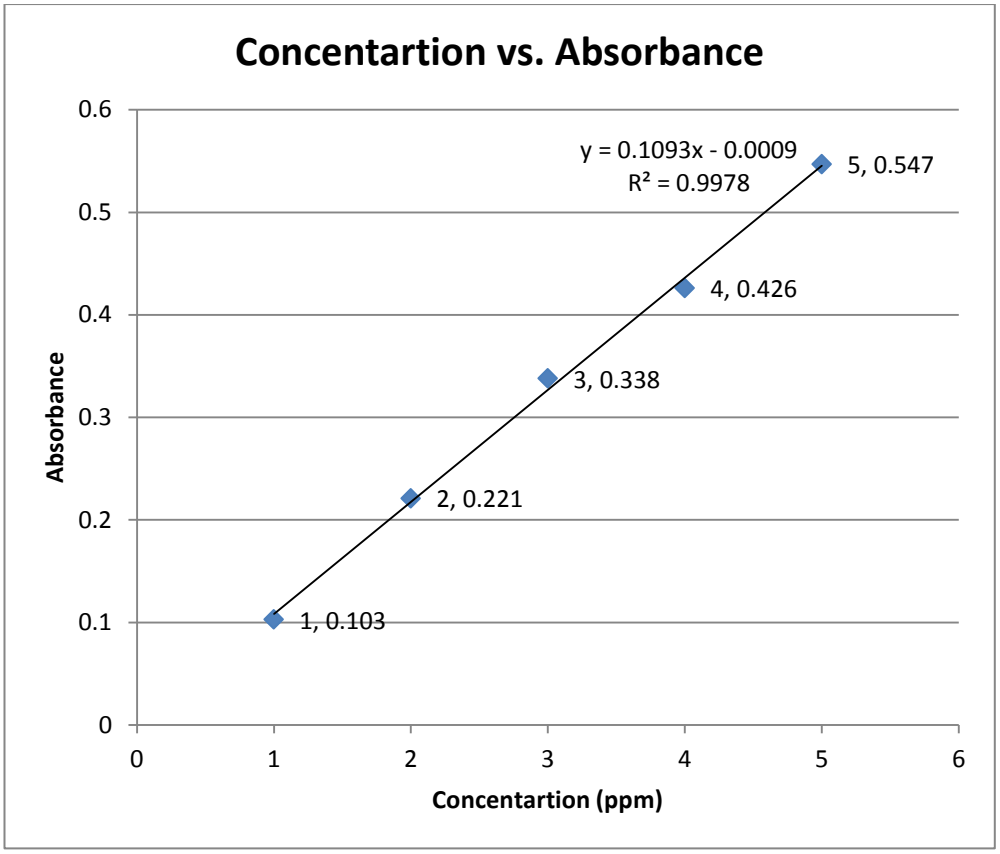

Figure 4.21 Calibration curve for methyl orange.

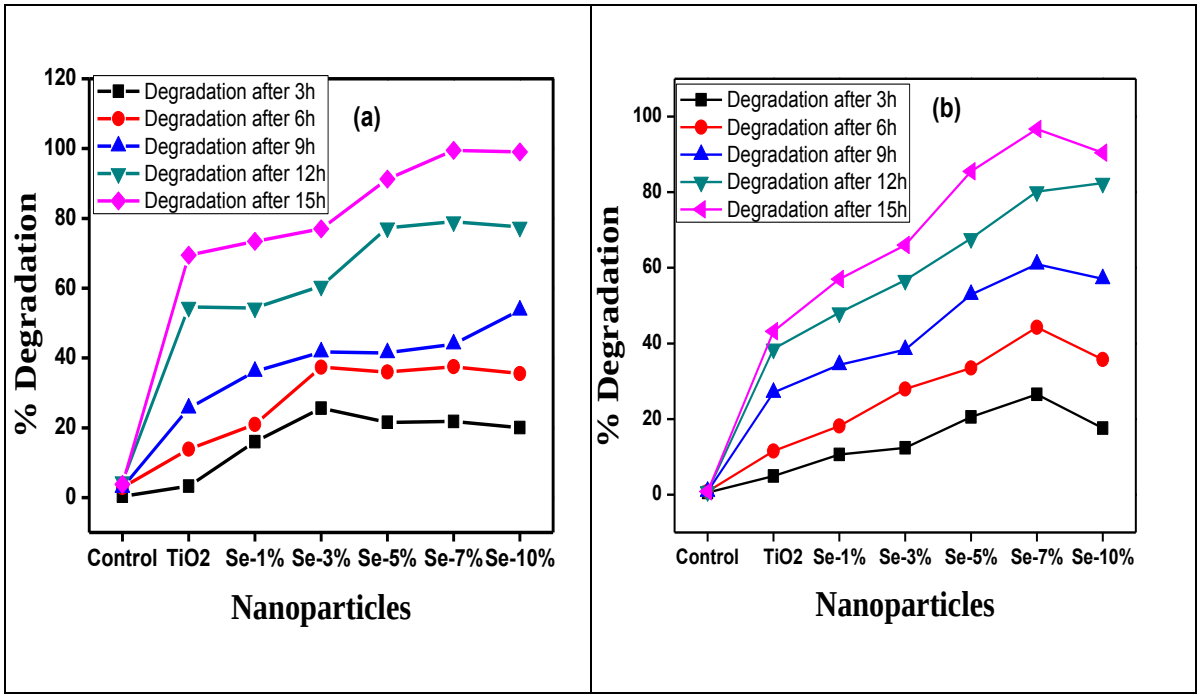

Figure 4.22 Efficiency of (a) Cu and (b) Se doped samples for methyl orange degradation.

4.5 Comparison of Cu & Se Doped Best Catalysts

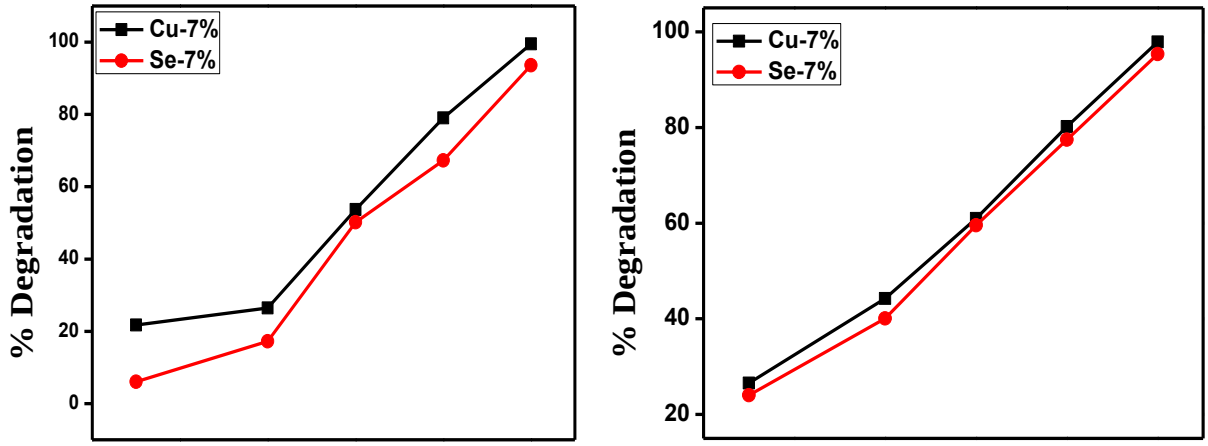

(a) Degradation of glyphosate

(b) Degradation of methyl orange orange

Figure 4.23 Comparison of (a) Cu-7% and (b) Se-7% efficiency.

To determine the concentration from absorbance of nano catalysts calibration curve was drawn **fig 4.19** and **4.21** by taking concetartions of 1, 2, 3, 4 and 5 ppm. Calibration curve shows R2 value near to unity which is very close to unity showing that curve has minimum chances of error. From theses curves the conecntartion was determined and efficiency graphs were plotted shown in **fig 4.23** it was observed that Cu-7% and Se-7% were more efficient than all other doped catalysts. After determining the concentration from curve efficiency of each catalyst was determined. Efficiency of pure TiO_2 is very less but in comparison the doped catalysts were very efficient in degradation. Best efficiency was shown by catalysts having 7% dopant concentration which is 97%. Efficiency was determined by using the following equation

$$\text{Efficiency} = A^0 - At / A^0 \times 100$$

Both th best catalysts were compared together as shown in **fig 4.23** nad it was observed that Cu-7% was best of all for photocatalytic degradations.

4.6 Reuseabaility of Cu-7% doped TiO_2 nanocatalyst

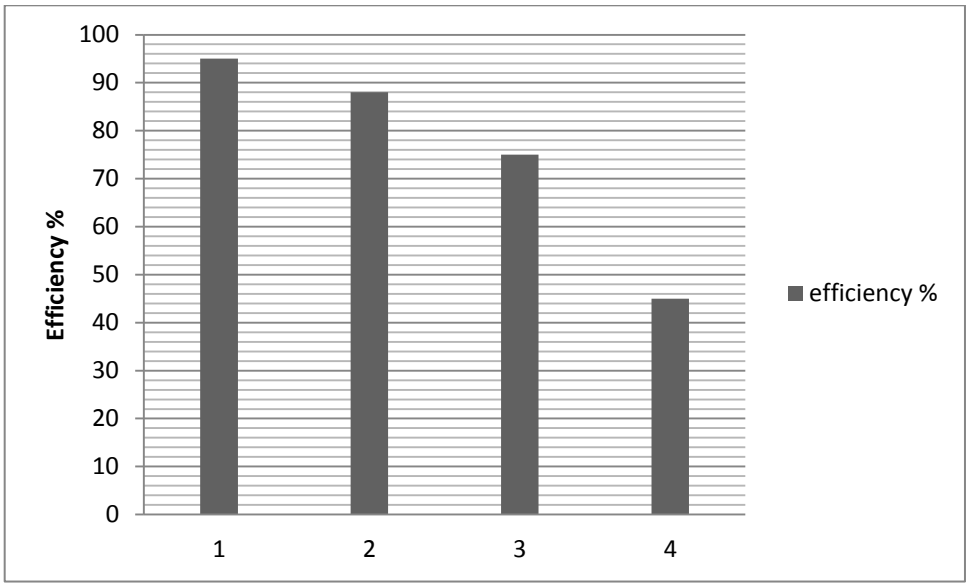

Figure 4.24 Plot of re-useability of nanocatalysts

To check reuseability catalyst used for first time were 97% efficient after that their efficiency was decreased as shown in **fig 4.24** but can be reused at least 4 times, in last use they were taking more time for degradation.

Chapter 5: Conclusion

Sol-gel method was adopted to synthesize pure TiO_2 particles and doped with Cu and Se ions. 5 catalysts from each dopant was prepared by varying the amount of dopant. XRD results showed that all the peaks are attributed to pure anatase tetragonal having different crystallite size ranging from 22-12 nm. The crystallite size decreases as the dopant concentration was increased. SEM analysis showed morphology of TiO_2 as irregular spherical but doping cause a change in morphology as it becomes irregular or more like aggregated plates. Loading more dopant also increases the surface area of particles. Cu-7% and Se-7% have highest surface area of 59.32 and 80.23 m^2/g respectively because the particles are well dispersed and have less chances of agglomeration. The optical properties were measured by tauc plot the doping lowers the band gap increasing the photocatalytic activity. Degradation of methyl orange and glyphosate was done to check weather the catalyst are efficient or not. The highest efficiency was with 7% Cu that is 97% after 15 hours of irradiation with visible light. The degradation can be attributed to the presence of hydroxyl ions on the surface of TiO_2. The comparison of efficiency of Cu-7% and Se-7% shows that Cu-7% is slightly more active than Se-7%.

Chapter 6: References

[1] M. Younger, H. R. Morrow-Almeida, S. M. Vindigni, and A. L. Dannenberg, "The Built Environment, Climate Change, and Health Opportunities for Co-Benefits," *American Journal of Preventive Medicine,* vol. 35, pp. 517-526, Nov 2008.

[2] D. Coley and T. Kershaw, "Changes in internal temperatures within the built environment as a response to a changing climate," *Building and Environment,* vol. 45, pp. 89-93, Jan 2010.

[3] M. Varavipour, T. Asadi, and M. Mashal, "Application of two layers of soil with different textures for decreasing pollution from landfills to the subterranean water table," *Research on Crops,* vol. 12, pp. 833-838, Dec 2011.

[4] M. Regadio, A. I. Ruiz, M. Rodriguez-Rastrero, and J. Cuevas, "Containment and attenuating layers: An affordable strategy that preserves soil and water from landfill pollution," *Waste Management,* vol. 46, pp. 408-419, Dec 2015.

[5] T. G. Kazi, M. B. Arain, M. K. Jamali, N. Jalbani, H. I. Afridi, R. A. Sarfraz*, et al.*, "Assessment of water quality of polluted lake using multivariate statistical techniques: A case study."

[6] A. Azizullah, M. N. K. Khattak, P. Richter, and D.-P. Häder, "Water pollution in Pakistan and its impact on public health — A review."

[7] D. M. H. Talhat Munir, Sana Naseem, "Water Pollution-A Menace of Freshwater Biodiversity: A Review" 2016.

[8] L. J. PUCKETT, "Identifying the Major Sources of Nutrient Water Pollution," 1995.

[9] Rebecka Törnqvista., "Health risks from large-scale water pollution: Trends in Central Asia," vol. 37, pp. 435-442, February 2011.

[10] I. Wesstrom, A. Joel, and I. Messing, "Controlled drainage and subirrigation - A water management option to reduce non-point source pollution from agricultural land," *Agriculture Ecosystems & Environment,* vol. 198, pp. 74-82, Dec 15 2014.

[11] B. E. Rittmann, "Aerobic biological treatment " vol. 2, 1987.

[12] D. Bahnemann, "Photocatalytic water treatment: solar energy applications" pp. 445–459, 2004.

[13] E. J. Bouwer and P. B. Crowe, "Biological Processes in Drinking-Water Treatment," *Journal American Water Works Association,* vol. 80, pp. 82-93, Sep 1988.

[14] S. R.S.Barhate, "Nanofibrous filtering media: Filtration problems and solutions from tiny materials," vol. 296, pp. 1-8, 15 June 2007.

[15] A. W. G.M.McLaughlin, .K.D.Hauffe, "Capillary electrophoresis methods development and sensitivity enhancement strategies for the separation of industrial and environmental chemicals," vol. 744, pp. 123-134, September 1996.

[16] Santiago Esplugas, Jaime Giménez, Sandra Contreras, Esther Pascual, and Miguel Rodríguez, "Comparison of different advanced oxidation processes for phenol degradation," vol. 36, pp. 1034-1042, February 2002.

[17] K. Soutsas, V. Karayannis, I. Poulios, A. Riga, K. Ntampegliotis, X. Spiliotis*, et al.*, "Decolorization and degradation of reactive azo dyes via heterogeneous photocatalytic processes," *Desalination,* vol. 250, pp. 345-350, Jan 1 2010.

[18] R. P. Suri, H. M. Thornton, and M. Muruganandham, "Disinfection of water using Pt- and Ag-doped TiO_2 photocatalysts," *Environ Technol,* vol. 33, pp. 1651-9, Jul-Aug 2012.

[19] J. Wang, R. H. Li, Z. H. Zhang, X. D. Zhang, W. Sun, H. Wang*, et al.*, "Photocatalytic degradation of dyestuff wastewater under visible light irradiation using micron-sized mixed

crystal TiO_2 powders," *Journal of Chemical Technology and Biotechnology,* vol. 82, pp. 588-597, Jun 2007.

[20] M. B. Suwarnkar, R. S. Dhabbe, A. N. Kadam, and K. M. Garadkar, "Enhanced photocatalytic activity of Ag doped TiO_2 nanoparticles synthesized by a microwave assisted method," *Ceramics International,* vol. 40, pp. 5489-5496, 2014.

[21] V. Augugliaro, C. Baiocchi, A. B. Prevot, M. C. Brussino, E. Garcia-Lopez, V. Loddo*, et al.*, "Sunlight photocatalytic degradation of azo-dyes in aqueous suspension of polycrystalline TiO_2," *Fresenius Environmental Bulletin,* vol. 11, pp. 459-465, Aug 2002.

[22] G. S. M. T. Manoj, "A review of TiO_2 nanoparticles" vol. 56, pp. 1639–1657, November 21, 2010.

[23] V. Diesen, C. W. Dunnill, E. Osterberg, I. P. Parkin, and M. Jonsson, "Silver enhanced TiO_2 thin films: photocatalytic characterization using aqueous solutions of tris(hydroxymethyl)aminomethane," *Dalton Transactions,* vol. 43, pp. 344-351, 2014.

[24] V. V. Afanas'ev, "Electron Band Alignment at Interfaces of Semiconductors with Insulating Oxides: An Internal Photoemission Study," *Advances in Condensed Matter Physics,* vol. 2014, p. 30, 2014.

[25] S. Anandan and M. Miyauchi, *Photocatalytic Activity of Cu^{2+}-Grafted Metal-Doped ZnO Photocatalysts Under Visible-Light Irradiation* vol. 79, 2011.

[26] S. Burnside, J.-E. Moser, K. Brooks, M. Grätzel, and D. Cahen, "Nanocrystalline Mesoporous Strontium Titanate as Photoelectrode Material for Photosensitized Solar Devices: Increasing Photovoltage through Flatband Potential Engineering," *The Journal of Physical Chemistry B,* vol. 103, pp. 9328-9332, 1999/10/01 1999.

[27] B. B. Yu, J. B. Zeng, L. F. Gong, M. S. Zhang, L. M. Zhang, and X. Chen, "Investigation of the photocatalytic degradation of organochlorine pesticides on a nano-TiO_2 coated film," *Talanta,* vol. 72, pp. 1667-1674, Jul 31 2007.

[28] S. F. Chen and G. Y. Cao, "Photocatalytic degradation of organophosphorus pesticides using floating photocatalyst TiO_2 center dot SiO_2/beads by sunlight," *Solar Energy,* vol. 79, pp. 1-9, 2005.

[29] M. Myilsamy, M. Mahalakshmi, V. Murugesan, and N. Subha, "Enhanced photocatalytic activity of nitrogen and indium co-doped mesoporous TiO_2 nanocomposites for the degradation of 2,4-dinitrophenol under visible light," *Applied Surface Science,* vol. 342, pp. 1-10, Jul 1 2015.

[30] X. Xu, F. Ji, Z. Fan, and L. He, "Degradation of glyphosate in soil photocatalyzed by $Fe_3O_4/SiO_2/TiO_2$ under solar light," *Int J Environ Res Public Health,* vol. 8, pp. 1258-70, Apr 2011.

[31] S. Raut-Jadhav, D. V. Pinjari, D. R. Saini, S. H. Sonawane, and A. B. Pandit, "Intensification of degradation of methomyl (carbamate group pesticide) by using the combination of ultrasonic cavitation and process intensifying additives," *Ultrason Sonochem,* vol. 31, pp. 135-42, Jul 2016.

[32] K. Tanaka, S. M. Robledo, T. Hisanaga, R. Ali, Z. Ramli, and W. A. Bakar, "Photocatalytic degradation of 3,4-xylyl N-methylcarbamate (MPMC) and other carbamate pesticides in aqueous TiO_2 suspensions," *Journal of Molecular Catalysis a-Chemical,* vol. 144, pp. 425-430, Aug 19 1999.

[33] S. F. Chen, M. Y. Zhao, and Y. W. Tao, "Photocatalytic degradation of organophosphoros pesticides using TiO_2 supported on fiberglass," *Microchemical Journal,* vol. 54, pp. 54-58, Jul 1996.

[34] K. Umar, A. Aris, H. Ahmad, T. Parveen, J. Jaafar, Z. A. Majid*, et al.*, "Synthesis of visible light active doped TiO_2 for the degradation of organic pollutants—methylene blue and glyphosate," *Journal of Analytical Science and Technology,* vol. 7, 2016.

[35] P. Kongsong, L. Sikong, S. Niyomwas, and V. Rachpech, "Photocatalytic Degradation of Glyphosate in Water by N-Doped SnO_2/TiO_2 Thin-Film-Coated Glass Fibers," *Photochemistry and Photobiology,* vol. 90, pp. 1243-1250, Nov-Dec 2014.

[36] S. F. Chen and Y. Z. Liu, "Study on the photocatalytic degradation of glyphosate by TiO_2 photocatalyst," *Chemosphere,* vol. 67, pp. 1010-1017, Mar 2007.

[37] B. Michael, T. Meyer, K. A. Loftin, E. A. Lee, G. H. Hinshaw, J. E. Dietze*, et al.*, "Determination of Glyphosate, its Degradation Product Aminomethylphosphonic Acid, and Glufosinate, in Water by Isotope Dilution and Online Solid-Phase Extraction and Liquid Chromatography/Tandem Mass Spectrometry," *U.S. Geological Survey,* 2009.

[38] L. H, J. SR, and J. DP, "Degradation and Isotope Source Tracking of Glyphosate and Aminomethylphosphonic Acid," *J Agric Food Chem,* vol. 64, 2016 Jan 13.

[39] L. Y. Chen Shifu, "Study on the photocatalytic degradation of glyphosate by TiO_2 photocatalyst," *scinece direct* vol. 67, pp. 1010–1017, 2006.

[40] B. freedman, "Controversy over the use of herbicides in forestry, with particular reference to glyphosate usage," *Environmental Carcinogenesis Reviews* vol. 8, 1990

[41] J. Q. Chen, Z. J. Hu, and N. X. Wang, "Photocatalytic mineralization of glyphosate in a small-scale plug flow simulation reactor by UV/TiO_2," *Journal of Environmental Science and Health Part B-Pesticides Food Contaminants and Agricultural Wastes,* vol. 47, pp. 579-588, 2012.

[42] J. P. Naomi L. Stock , K. Vinodgopal , and Prashant V. Kamat "Combinative Sonolysis and Photocatalysis for Textile Dye Degradation " *Environ. Sci. Technol.,* vol. 34, pp. 1747–1750, 2000.

[43] T. V. L. Thejaswinia, D. Prabhakarana, prabhakaran, and M. A. Maheswarib, "Soft Synthesis of Bi Doped and Bi-N Co-doped TiO_2 Nanocomposites: A Comprehensive Mechanistic Approach towards Visible Light Induced Ultra-Fast Photocatalytic Degradation of Fabric Dye Pollutant," 22-1-2016.

[44] M. P. Volume Issue 1, CeciliaBaraldi. Jeannette JacquelineŁucejko "Colour fading in textiles: A model study on the decomposition of natural dyes," vol. 85,, pp., Pages 174-182, January 2007.

[45] H. Koohestani and S. K. Sadrnezhaad, "Photocatalytic degradation of methyl orange and cyanide by using TiO_2/CuO composite."

[46] S. Xie, P. Huang, J. J. Kruzic, X. Zeng, and H. Qian, "A highly efficient degradation mechanism of methyl orange using Fe-based metallic glass powders," vol. 6, p. 21947, 02/23/online 2016.

[47] X. Q. Min Liu, Masahiro Miyauchi, and Kazuhito Hashimoto, "Cu(II) Oxide Amorphous Nanoclusters Grafted Ti^{3+} Self-Doped TiO_2: An Efficient Visible Light Photocatalyst," vol. 23, p. 5282−5286, 2011.

[48] V. K. Chrysanthi Berberidou, Eleutheria Kazala,Dimitra A. Lambropoulou, Athanasios Kouras, Christina I. Kosma,Triantafyllos A. Albanis, Ioannis Pouliosa, "Study of the decomposition and detoxification of the herbicidebentazon by heterogeneous photocatalysis: Kinetics, intermediatesand transformation pathways," pp. 150–163, 2016.

[49] M. C. Augustine Chioma Affam, "Degradation of pesticides chlorpyrifos, cypermethrin and chlorothalonil in aqueous solution by TiO_2 photocatalysis," vol. 130 pp. 160-165, 2013.

[50] L. A. S. Murtaza Sayed, Javed Ali Khan, Noor S. Shah,Jan Nisar, and P. Z. Hasan M. Khan, and Abdur Rahman Khan, "Efficient Photocatalytic Degradation of Norfloxacin in Aqueous Media by Hydrothermally Synthesized Immobilized TiO_2/Ti Films with Exposed {001} Facets," vol. 120, p. 9916−9931, 2016.

[51] H. P. Jina Choi, and Michael R. Hoffmann, "Effects of Single Metal-Ion Doping on the Visible-Light Photoreactivity of TiO_2," vol. 114, pp. 783–792, 2009.

[52] M. B. Suwarnkar, R.S.Dhabbe, A.N.Kadam, and K.M.Garadkarn, "Enhanced photocatalytic activity of Ag doped TiO_2 nanoparticles synthesized by a microwave assisted method," vol. 137, pp. 5489–5496, 2013.

[53] Mendiola-Alvarez, S. Y. Guzmán-Mar, J. L. Turnes-Palomino, Maya-Alejandro, Hernández-Ramírez, and Hinojosa-Reyes, "UV and visible activation of Cr(III)-doped TiO_2 catalyst prepared by a microwave-assisted sol–gel method during MCPA degradation," *Environmental Science and Pollution Research,* vol. 24, pp. 12673-12682, 2016.

[54] C. F. J. Choinaa, G.-U. Flechsig, H. Kosslick, V.A. Tuand, N.D. Tuyend,N.A. Tuyend, A. Schulza,, "Photocatalytic properties of Zr-doped titania in the degradation of thepharmaceutical ibuprofen," vol. 274, pp. 108– 116, 2014.

[55] R. Yuana, B. Zhoua, D. Huaa, and C. Shia, "Enhanced photocatalytic degradation of humic acids using Al and Fe co-doped TiO_2 nanotubes under UV/ozonation for drinking water purification."

[56] A. N. Banerjee, S. Joo, and Bong-KiMin, "Photocatalytic Degradation of Organic Dye by Sol-Gel-Derived Gallium-Doped Anatase Titanium Oxide Nanoparticles for Environmental Remediation."

[57] A. N. Kadam, R. S. Dhabbe, M. R. Kokate, Y. B. Gaikwad, and K. M. Garadkar, "Preparation of N doped TiO_2 via microwave-assisted method and its photocatalytic activity for degradation of Malathion," pp. 669–676, 2014.

[58] R. Rahimi, S. S. Moghaddam, and M. Rabbani, "Comparison of photocatalysis degradation of 4-nitrophenol using N,S co-doped TiO_2 nanoparticles synthesized by two different routes," vol. 64, pp. 17–26, 2012.

[59] K. Pathakoti, S. Morrow, C. Han, M. Pelaez, X. He, D. D. Dionysiou*, et al.*, "Photoinactivation of Escherichia coli by Sulfur-Doped and Nitrogen−Fluorine-Codoped TiO_2 Nanoparticles under Solar Simulated Light and Visible Light Irradiation."

[60] A. Eslami, MostafaMAmini, A. R. Yazdanbakhsh, Anoushiravan, Mohseni-Bandpei, A. A. Safarid*, et al.*, "N,S co-doped TiO_2 nanoparticles and nanosheets in simulated solar light for photocatalytic degradation of non-steroidal anti-inflammatory drugs in water: a comparative study," vol. 91, pp. 2693–2704, 2016.

[61] L. D. Than, N. S. Luong, V. D. Ngo, N. M. Tien, T. N. Dung, N. M. Nghia*, et al.*, "Highly Visible Light Activity of Nitrogen Doped TiO_2 Prepared by Sol–Gel Approach," *Journal of Electronic Materials,* vol. 46, pp. 158-166, 2016.

[62] M. Antonopoulou, A. Giannakas, F. Bairamis, M. Papadaki, and I. Konstantinou, "Degradation of organophosphorus flame retardant tris (1-chloro-2-propyl) phosphate (TCPP) by visible light N,S-codoped TiO_2 photocatalysts."

[63] R. L. A. Pérez-Larios , A. Hernández-Gordillo , F. Tzompantzi , R. Gómez , L.M. Torres-Guerra, "Improved hydrogen production from water splitting using TiO_2–ZnO mixed oxides photocatalysts," vol. 100 pp. 139–143, 2012.

[64] H. Hossaini, G. Moussavi, and M. F. rokhi, "The investigation of the LED-activated FeFNS-TiO_2 nanocatalyst for photocatalytic degradation and mineralization of organophosphate pesticides in water," vol. 59, pp. 130-144, 2014

[65] M. A. Barakat, R. I. Al-Hutailah, E. Qayyum, J. Rashid, and J. N. Kuhn, "Pt nanoparticles/TiO_2 for photocatalytic degradation of phenols in wastewater."

[66] S. Dominguez, M. Huebra, C. Han, P. Campo, M. N. Nadagouda, M. J. Rivero*, et al.*, "Magnetically recoverable TiO_2-WO_3 photocatalyst to oxidize bisphenol A from model wastewater under simulated solar light," *Environ Sci Pollut Res Int,* pp. 12589-12598, 2016.

[67] Y. Tang, W. Di, X. Zhai, R. Yang, and W. Qin, "NIR-Responsive Photocatalytic Activity and Mechanism of $NaYF_4$:Yb,Tm@TiO_2 Core−Shell Nanoparticles."

[68] A. Cordero-García, G. T. Palomino, L. Hinojosa-Reyes, J. L. Guzmán-Mar, L. Maya-Teviño, and A. Hernández-Ramírez, "Photocatalytic behaviour of WO_3/TiO_2-N for diclofenac degradation using simulated solar radiation as an activation source," 2016.

[69] M. A. Habib, M. T. Shahadat, N. M. Bahadur, I. M. I. Ismail, and A. J. Mahmood, "Synthesis and characterization of ZnO-TiO_2 nanocomposites and their application as photocatalysts."

[70] M. J. Muñoz-Batista, M. N. Gómez-Cerezo, A. Kubacka, D. Tudela, and a. Fernández-García, "Role of Interface Contact in CeO_2–TiO_2 Photocatalytic Composite Materials."

[71] J. Wang, H. Ruan, W. Li, D. Li, Y. Hu, J. Chen*, et al.*, "Highly Efficient Oxidation of Gaseous Benzene on Novel Ag_3VO_4/TiO_2 Nanocomposite Photocatalysts under Visible and Simulated Solar Light Irradiation."

[72] V. Stengl, T. Matys Grygar, J. Velicka, J. Henych, and S. Bakardjieva, "Impact of Ge^{4+} Ion as Structural Dopant of Ti^{4+} in Anatase: Crystallographic Translation, Photocatalytic Behavior, and Efficiency under UV and VIS Irradiation," *Journal of Nanomaterials,* 2012 2012.

[73] B. A. Bhanvase, T. P. Shende, and S. H. Sonawane, "A review on graphene–TiO_2 and doped graphene–TiO_2 nanocomposite photocatalyst for water and wastewater treatment," vol. 6 pp. 1–14.

[74] X. Liu, H. Hong, X. Wu, Y. Wu, Y. Ma, W. Guan*, et al.*, "Synthesis of TiO_2–Reduced Graphene Oxide Nanocomposites for Efficient Adsorption and Photodegradation of Herbicides," *Water, Air, & Soil Pollution,* vol. 227, 2015.

[75] N. Yang, Y. Liu, HaoWen, Z. Tang, H. Zhao, Y. Li*, et al.*, "Photocatalytic Properties of Graphdiyne and Graphene Modified TiO_2: From Theory to Experiment."

[76] K. Umar, A. Aris, H. Ahmad, T. Parveen, J. Jaafar, Z. A. Majid*, et al.*, "Synthesis of visible light active doped TiO_2 for the degradation of organic pollutants—methylene blue and glyphosate," vol. 7, p. 29, 2016.

[77] D. R. R. Vignesh C. Bhethanabotla, John N. Kuhna, "Assessment of mechanisms for enhanced performance ofYb/Er/titania photocatalysts for organic degradation: Role of rareearth elements in the titania phase," vol. 202, pp. 156–164, 2017.

[78] A. C.-L. M. Salazar-Villanueva, A.A. Zaldívar-Cadena, A. Tovar-Corona, and O. V.-C. M.L. Guevara-Romero, "Effect of the electronic state of Ti on M-doped TiO_2 nanoparticles (M=Zn, Ga or Ge) with high photocatalytic activities: A experimental and DFT molecular study," pp. 8–14, 2017.

[79] P. Singla, O. P. Pandey, and K. Singh, "Study of photocatalytic degradation of environmentally harmful phthalate esters using Ni-doped TiO_2 nanoparticles," vol. 13, pp. 849–856, 2016.

[80] A. S. Taranjeet Kaur, Amrit Pal Toor, R.K. Wanchoo, "Utilization of solar energy for the degradation of carbendazim and propiconazole by Fe doped TiO_2," vol. 125, pp. 65–76 2016.

[81] C. H. Javed Ali Khan, Noor S. Shah,Hasan M. Khan, Mallikarjuna N. Nadagouda, and P. F. Vlassis Likodimos, Kevin O'Shea, and Dionysios D. Dionysiou, "Ultraviolet–Visible Light–Sensitive High Surface Area Phosphorous-Fluorine–Co-Doped TiO_2 Nanoparticles for the Degradation of Atrazine in Water," vol. 31, 2014.

[82] T. K. Romina Zˇ abar , Jure Fabjan , Mojca Bavcon Kralj , Polonca Trebš, "Photocatalytic degradation with immobilised TiO_2 of three selected neonicotinoid insecticides: Imidacloprid, thiamethoxam and clothianidin".

[83] S. M. El-Sheikh, T. M. Khedr, A. Hakki, A. A. Ismail, W. A. Badawy, and D. W. Bahnemann, "Visible light activated carbon and nitrogen co-doped mesoporous TiO_2 as efficient photocatalyst for degradation of ibuprofen," *Separation and Purification Technology,* vol. 173, pp. 258-268, 2017.

[84] M. M. Ali Bumajdad and M. E.-K. Yasser Abdel-Moneam, "Nanostructured mesoporous Au/TiO_2 for photocatalytic degradation of a textile dye: the effect of size similarity of the deposited Au with that of TiO_2 pores," vol. 49, pp. 1743–1754, 2014.

[85] M. Antonopoulou, A. Giannakas, F. Bairamis, M. Papadaki, and I. Konstantinou, "Degradation of organophosphorus flame retardant tris (1-chloro-2-propyl) phosphate (TCPP) by visible light N,S-codoped TiO_2 photocatalysts," *Chemical Engineering Journal,* vol. 318, pp. 231-239, 2017.

[86] G. Colón, M. Maicu, M. C. Hidalgo, and J. A. Navío, "Cu-doped TiO_2 systems with improved photocatalytic activity," *Applied Catalysis B: Environmental,* vol. 67, pp. 41-51, 2006.

[87] M. Khairy and W. Zakaria, "Effect of metal-doping of TiO_2 nanoparticles on their photocatalytic activities toward removal of organic dyes," Received 18 December 2013; accepted 15 January 2014.

[88] A. Cordero-Garcia, G. Turnes Palomino, L. Hinojosa-Reyes, J. L. Guzman-Mar, L. Maya-Tevino, and A. Hernandez-Ramirez, "Photocatalytic behaviour of WO_3/TiO_2-N for diclofenac degradation using simulated solar radiation as an activation source," *Environ Sci Pollut Res Int,* vol. 24, pp. 4613-4624, Feb 2017.

[89] L. G. Devi, R. Kavitha, and B. Nagaraj, "Bulk and surface modification of TiO_2 with sulfur and silver: Synergetic effects of dual surface modification in the enhancement of photocatalytic activity," *Materials Science in Semiconductor Processing,* vol. 40, pp. 832-839, Dec 2015.